FACULTY OF SCIENCE AND TECHNOLOGY

BACHELOR'S THESIS

Study programme / specialization:	The Spring semester, 2024
Biological Chemistry	**Open** / Confidential

Author: Renate Paulsen Nygård

Supervisor at UiS: Hanne Røland Hagland

Co-supervisor: Julie Nikolaisen

Thesis title:

Growth assessment of pancreatic ductal adenocarcinoma Panc-1 cell line in collagen and alginate of different mechanical properties.

Credits: 20 ECTS

Keywords:
Stroma, Pancreatic cancer, Extracellular matrix (ECM), Collagen, Alginate, Tumor Microenvironment, Mechanical properties of alginate

Pages: 42
+ appendix: 11

Stavanger, May 14, 2024

Approved by the Dean 30 Sep 21
Faculty of Science and Technology

Acknowledgements

I would like to express my sincere gratitude to Professor Hanne R. Hagland for her invaluable advice and guidance throughout the course of this research. Her expertise and insight have significantly shaped the trajectory and outcomes of this study.

I would like to extend my sincere thanks to Julie Nikolaisen for her excellent training and invaluable assistance in the laboratory.

My heartfelt thanks go out to my family and children for their unwavering support and encouragement. Their patience and understanding have been a source of strength and inspiration during this academic journey.

I am also very grateful to Birgitte, Vilde, Vickie, and Nadiira, my fellow students in group room C-164. Their support and teamwork made this experience productive and enjoyable.

Abstract

This thesis explored the effects of varying concentrations of collagen and alginate on the growth of the Panc-1 pancreatic cancer cell line.
The research employs 3D culturing techniques to simulate the tumor microenvironment, using collagen and alginate as substrates to modulate the physical stress exerted on the cells. By adjusting the concentrations of these biopolymers, the study replicates various stiffness levels that mimic the natural stiffness found within the human body. The primary methods utilized include rheological measurements to determine the mechanical properties of the alginate gels and resazurin assays to assess cell viability.

Results indicate that Panc-1 cells exhibit distinct proliferative behaviors in response to the different mechanical stresses induced by the biopolymer matrices. Cells cultured in lower alginate concentrations demonstrated enhanced proliferation and viability, suggesting that softer matrices are more conducive to cell growth. In contrast, the response of cells in collagen matrices was more complex, with varying effects on cell proliferation observed across different stiffness levels.

The findings highlight the potential of manipulating ECM properties to influence cancer cell behavior and suggest that altering matrix stiffness could be a viable approach to understand more of how the stroma affects cancer cells in pancreatic cancer.

List of figures

List of tables

Abbreviations

ATCC	American Type Culture Collection
CAFs	Cancer Associated Fibroblasts
DMEM	Dulbecco´s Modification of Eagles Medium
ECM	Extracellular Matrix
EDC	N-(3-Dimethylaminopropyl)-N`-ethylcarbodiimide-hydrochloride
FBS	Fetal Bovine Serum
PBS	Phosphate Buffered Saline
PDAC	Pancreatic Ductal Adenocarcinoma
RGD	Arginine-Glycine-Aspartic acid

Contents

1 Introduction

Cancer remains one of the most challenging diseases to treat, with pancreatic cancer being particularly aggressive and resistant to conventional therapies (1). Recent research suggests that the physical properties of the tumor microenvironment can significantly influence cancer cell behavior, impacting both growth and metabolic pathways (2). It is therefore of interest to better understand cancer growth properties in terms of physical stress imposed by their growth conditions.

1.1 Cancer Biology

Cancer is a collective term for diseases marked by uncontrolled cell proliferation. These diseases range from benign tumors to malignant tumors, capable of infiltrating healthy tissues, and organs. Malignant cancer cells have the ability to metastasize, spreading to distant areas through the bloodstream or lymphatic system. The progression of the illness, chances of survival, and treatment approaches differ depending on the specific type of cancer (3-4). This thesis focuses on pancreatic cancer, a particularly dismal cancer disease with low survival rates and few treatment options.

Many solid tumors display characteristics such as self-sufficiency in growth signals, unrestricted cellular proliferation, continuous nutrient uptake, resistance to apoptosis, insensitivity to growth-inhibitory signals, and ability to invade and metastasize. Pancreatic Ductal Adenocarcinoma (PDAC) shares these traits (5).

1.2 Pancreas

The normal pancreas, illustrated in Figure 1-1, has a weight ranging from 100 to 150 grams, and a length between 12 and 15 centimeters, and is positioned at the farthest rear of the abdominal cavity, behind the stomach. The duodenum is in close proximity. The pancreas is divided into the head (*caput*), body (*corpus*), and tail (*cauda*) (6).

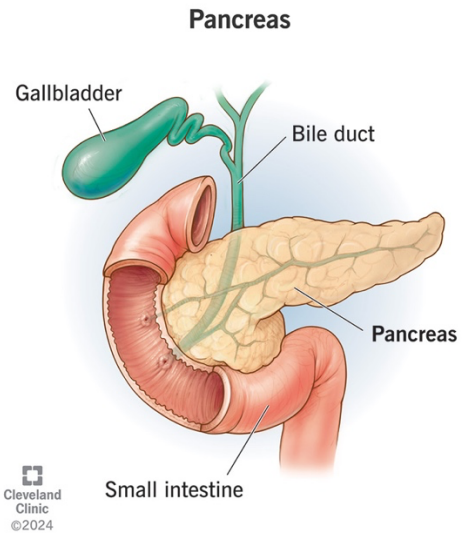

Figure 1-1: Illustration of a healthy pancreas in abdominal cavity (7).

The pancreas serves a dual role by producing pancreatic juice for digestion and hormones like insulin and glucagon, making it a gland with both exocrine and endocrine functions. In terms of digestion, the predominant portion of pancreatic tissue generates pancreatic juice, a digestive fluid. This constitutes the exocrine component of the pancreas, constituting roughly 95 percent of the total glandular tissue (8).

The endocrine part of the pancreas is arranged as discrete islets of Langerhans and contain five different endocrine cell types (beta, alpha, delta, upsilon, and epsilon). The endocrine cells in pancreas secrete five different hormones, among them insulin and glucagon (9). The pancreas gland manufactures approximately 1,5 liters of pancreatic juice daily, which is an alkaline fluid containing various enzymes essential for the digestion process (8).

1.3 Pancreatic Cancer

Pancreatic cancer is a lethal illness, mainly because of its tendency to be detected at advanced stages and its high resistance to chemotherapy and radiation therapy (10). There are very poor prognosis for this disease due to the cancers tendency to spread early throughout the body, and its aggressive local growth (11).

The prevalent form of pancreatic cancer is known as PDAC, illustration of tumor shown I Figure 1-2. Unfortunately, the available treatments are limited, predominantly consisting of palliative measures with various side effects (10).

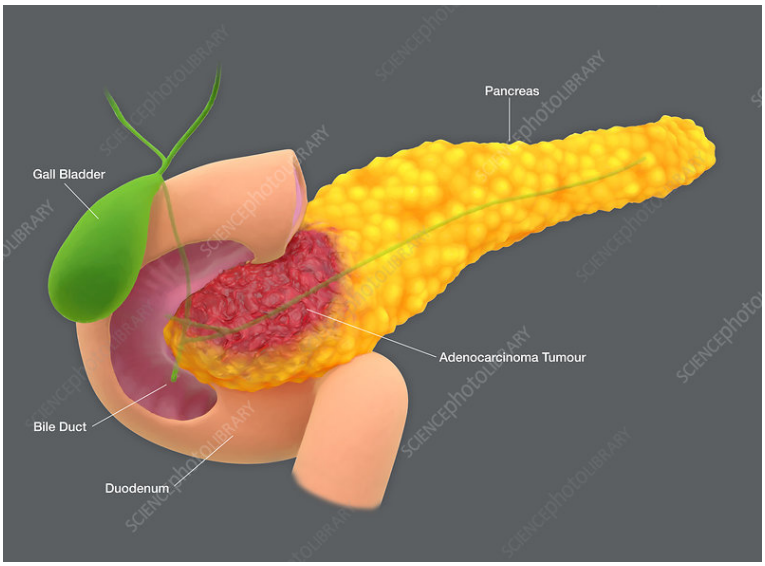

Figure 1-2: Illustration of pancreatic cancer tumor in head of pancreas (12).

Pancreatic cancer ranks as the tenth most prevalent cancer type in Norway for the individuals aged over 70. Symptoms are frequently nonspecific and may be linked to either local tumor expansion or the spread to distant organs. The primary symptoms encompass jaundice, reduced appetite, involuntary weight loss, and pain. In 2023, 1026 new cases of pancreatic cancer were diagnosed in Norway. The annual incidence has remained relatively stable since the 1990´s and the gender distribution is fairly equal. The incidence is highest in the age group of 65-75 years, but the disease can also occur in young adults. The median age at diagnosis is 72 years (13).

At the time of diagnosis there is a 5-year survival rate that stands at 10 %, with approximately 80-85 % of patients presenting either unresectable or metastatic disease. The prognosis is also poor for the small group of patients who are diagnosed with a localized resectable tumor, only 20 % survives 5 years after surgery (14).

As illustrated in Figure 1-3 which highlights the primary risk factors for pancreatic cancer, the majority of cases arise without a known cause. Despite this, old age clearly stands out as a predominant risk factor. In addition to these factors, there is an elevated risk among individuals who are obese, those with type 2 diabetes, and those with a history of chronic pancreatitis. Furthermore, hereditary predisposition is responsible for an estimated 10-15 % of pancreatic cancer cases (13).

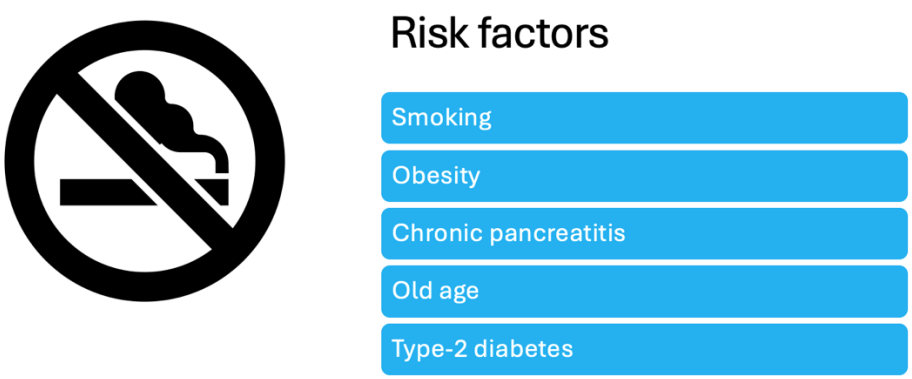

Figure 1-3: Illustration of the primary risk factors of pancreatic cancer.

1.4 Treatments

At present, surgery is the only option for achieving a cure for pancreatic cancer. Moreover, chemotherapy and radiation therapy are utilized, offering both palliative relief and potential life extending benefits (15). Complete tumor clearance often necessitates radical resection, especially for patients with borderline or locally advanced tumor. In recent decades, various surgical techniques and perioperative strategies have been developed to improve resectability and local tumor control. (16).

Pancreatic cancer is associated with a high degree of fibrosis, which impacts growth, treatment, and metastasis (17). This stromal impact is an area of considerable interest for ongoing and future research.

1.5 Extra Cellular Matrix (ECM)

1.5.1 Structure of ECM

The three-dimensional ECM, illustrated in Figure 1-4 is a network assembled with collagen, proteoglycans, elastin, fibronectin, laminins, and many other glycoproteins. These components interconnect, as well as bind to cell adhesion receptors, forming an intricate lattice within which cells are embedded across all tissues and organs. Receptors on the cell surface serve as transducers for signals from the ECM, orchestrating a range of cellular functions including growth, migration, survival and differentiation, these functions that are crucial for the maintenance of normal homeostasis (18).

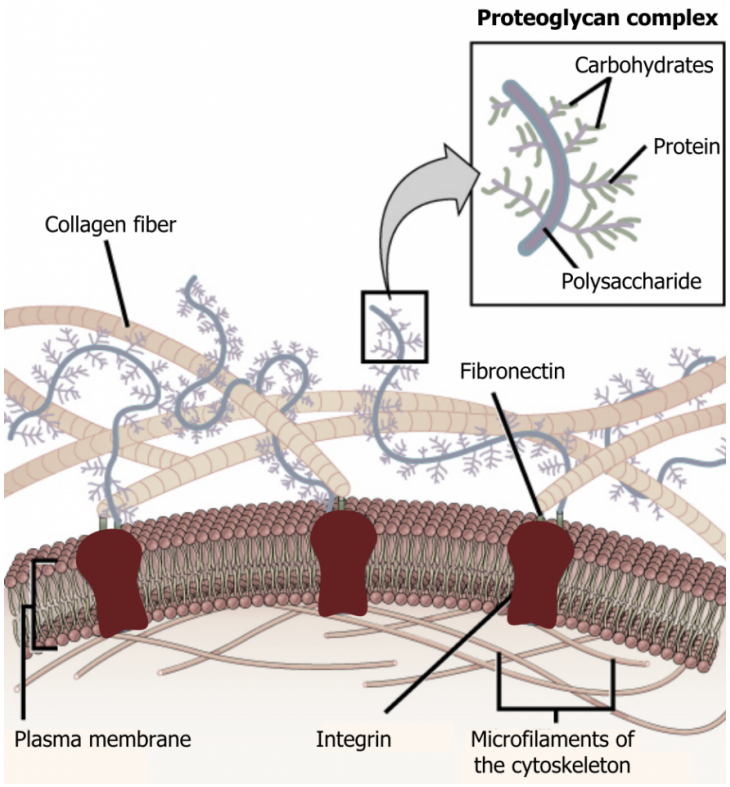

Figure 1-4: Illustration of the ECM. This is a network assembled with collagen, proteoglycans, elastin, fibronectin, laminins and many other glycoproteins (19).

1.5.2 Stiffness Affects Properties of ECM

Over the last twenty years, research has shown that the stiffness of the ECM affects crucial cellular activities like spreading, growth, and movement (20).

Researchers have commonly used elastic materials like polyacrylamide hydrogels or polydimethylsiloxane coated with ECM proteins, to study how stiffness influence cells (21). Initial studies highlighted the influence of substrate mechanics on cell structure and proliferation were often overshadowed by a focus on cellular genetics and biochemistry (20). However, this began to change in the late 1990s when Pelham and Wang, using polyacrylamide hydrogels of varying elasticities coated with ECM proteins, demonstrated that substrate stiffness significantly impact cell-ECM adhesion, spreading, and migration (22). The prevailing understanding is that cells use their internal structure to pull on their surroundings and can sense the stiffness of their environment through changes in how their surface proteins, like integrins gather and signal. As illustrated in Figure 1-5 the stiffness of the ECM plays a crucial role in coordinating growth, homeostasis, fostering repair mechanisms, and disease progression (20).

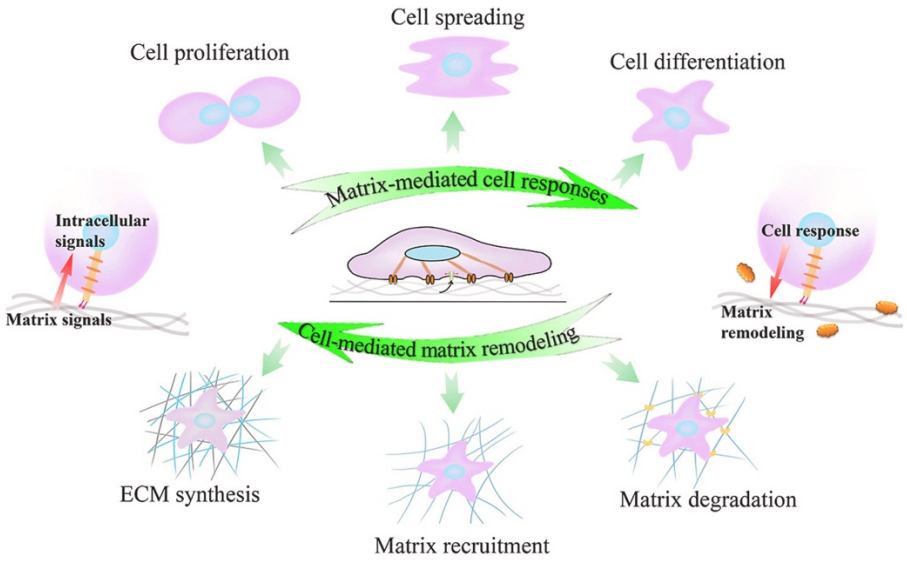

Figure 1-5: Illustration depicting the interaction between ECM and surrounding cells, emphasizing both matrix-mediated cellular responses and cell-driven matrix remodeling (23).

1.6 Stroma in Pancreatic Cancer

1.6.1 Distinctive Features

A distinctive feature of PDAC is the presence of desmoplasia-fibrotic change characterized by an overabundance of fibroblasts and the excessive deposition of ECM, which often makes up a significant portion of the tumor mass. In PDAC, there is a substantial increase in ECM deposition, with types I, III, and IV collagen being predominant in the structural framework of the PDAC ECM. Pancreatic cancer cells contribute to this fibrotic environment by prompting nearby fibroblasts to enhance the production of collagen, proteins, and fibronectin through paracrine signaling. This desmoplastic reaction is not only limited to primary tumor sites but is also observed in metastatic sites, characterized by significant increases in ECM elements such as hyaluronic acid and collagens, which within the tumor stroma of PDAC serve not merely as a static support, but also as a significant influencer on the behavior of cancer cells. This activity is involved in regulation of cancer cell proliferation, survival, and potential for metastasis (24).

One study found that with an increase in collagen I content in the ECM, pancreatic cancer cells transitioned from primarily utilizing glucose to predominantly relying on glutamine for metabolism. This indicates that a higher collagen density modifies the metabolic routes and nutritional needs of these cancer cells (25).

Another study revealed that type I collagen enhances the malignant characteristics of pancreatic cancer cells, such as their growth, survival, migration, and invasion capabilities. It

indicates that the dense collagen found in the desmoplastic reaction around pancreatic tumors fosters an environment that, although conducive to the tumor, is ultimately harmful to the host by facilitating tumor growth and spread (26).

1.6.2 Cancer Progression

Cancer progression in pancreas is associated with fibrotic stromal (desmoplastic) reaction, marked by a substantial deposition of ECM components, the enlistment and activation of cancer-associated fibroblasts (CAFs), and altered immune-surveillance. Remodeling of the stroma leads to altered interactions between tumor cells and stromal compartments, potentially fostering tumor progression (27).

Recent research has been focusing on therapeutically targeting this stroma to improve drug penetration. However, it is increasingly evident that the resilient stroma in pancreatic tumors serves not only as a barrier to drug delivery but also as a complex signaling partner that promotes tumorigenesis. Notably, pancreatic ductal adenocarcinoma stands out as one of the most stroma-rich cancers (28).

1.6.3 Modelling Cancer Growth-3D Culturing

Since the 1940´s, the standard approach to cell culture has been to grow cells on flat surfaces. This method is simple and supports cell survival well, but it fails to mimic the true three-dimensional environment found in tissues, where cells are encased by ECM. 3D cell cultures opposed to 2D, Figure 1-6, bring numerous benefits, especially for areas such as tumor research. In 3D settings, cells display behaviors and reactions that more accurately reflect their natural conditions, including their growth patterns, interactions, and response to various stimuli (29).

The cell line used in this thesis was Panc-1, derived from the pancreatic duct of a 56-year-old male patient. He was diagnosed with epithelioid carcinoma, and the cells exhibit adherent growth properties.

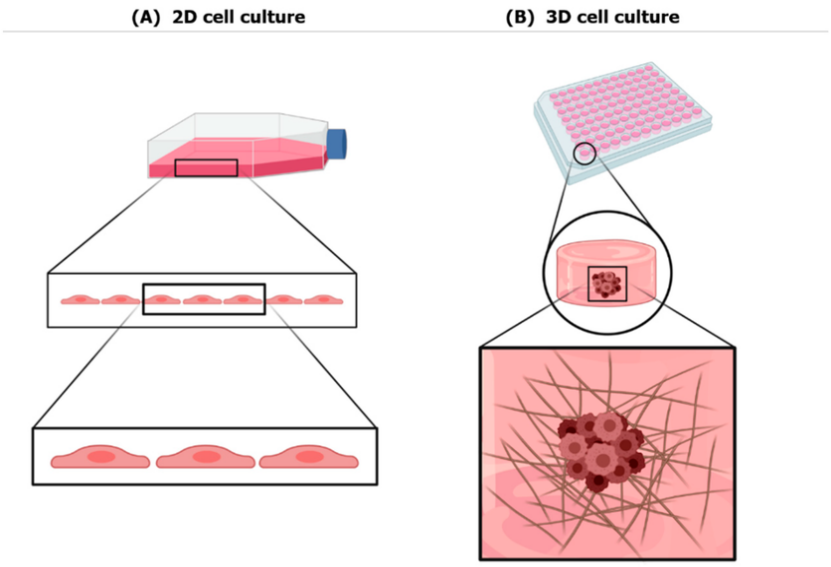

Figure 1-6: Cell Behavior in 2D (A) vs 3D (B) Cell Culture: Cells grown in traditional 2D culture typically adopt a flat shape that does not accurately reflect their natural physiological morphology. Cells cultured in 3D systems exist in a microenvironment that closely resembles in vivo conditions, allowing them to maintain a more representative morphology behavior (30).

1.7 Biopolymers Used in 3D Cancer Culturing

1.7.1 Effect of Rotenone on Cells in 3D Culturing

Rotenone is a commonly used organic pesticide. Its toxicity primarily arises from the inhibition of mitochondrial complex I, leading to oxidative stress, apoptosis, and decreased autophagy (31). In this project it was used to treat cells in one of the experiments.

1.7.2 Alginate in 3D Cell Culturing

Alginates are primarily derived from brown seaweeds, and used booth in the food and pharmaceutical industries (29). Alginates are naturally occurring anionic polysaccharides that are categorized as linear copolymers. They comprise of mainly two types of building blocks: mannuronic acid (M) and guluronic acid (G). These building blocks are linked together in a specific pattern, where mannuronic acid units have a specific ring shape known as 4C1, and guluronic acid units have a different ring shape known as 1C4. This structure allows alginates to perform unique functions, particularly in forming gels (32).

Natural polymers like alginate, can form hydrogels through various crosslinking techniques, including ionic and covalent bonding, using different methods to crosslink, like ionic or covalent crosslinking. Alginate exhibits a strong affinity for alkaline earth metals, promoting the formation of ionic hydrogels through interaction with divalent cations (29).

Stiffness of hydrogels play a significant role in cell behavior, one study found that lower concentrations of alginate tend to promote better cell proliferation and viability (33). Alginate hydrogels provide a 3D structure that resembles the ECM and have proven to be very effective and suitable for use in 3D cell cultures. Alginate is suitable material for this purpose due to its biocompatible properties, like the ability to fix cells within the matrix, and forming a gel-pore network that facilitates the diffusion of nutrients and waste materials. To ensure the production of hydrogels with uniform mechanical properties suitable for cell encapsulation, it is essential to use highly pure, well-characterized alginates (29).

Alginates does not contain natural ECM components like bioactive ligands and are therefore not chemically active. By attaching bioactive ligands, such as the cell adhesion motif Arginine-Glycine-Aspartic acid (RGD), to the hydrogel structure, the cell receptors can adhere to the hydrogel (34).

1.7.3 Collagen in 3D Cell Culturing

Collagen is primarily located in the skin and connective tissues, playing an essential role in maintaining the framework of the ECM. Collagen is a key structural protein, and known for its biocompatibility with living tissues, positive interactions with cells, and its natural ability to break down in the body. This crucial protein forms a triple helix structure that is central to its function (35). Biological matrices of collagen offers significant benefits, such as their inherent ability to adhere to cells, reliable stability within culture environment, and biophysical characteristics that closely mimic those found in living organisms (36).
In this thesis Telocol-10 bovine collagen was used due to its ideal properties in 3D culturing. The collagen is derived from an acid extraction process, producing a telopeptide-intact collagen composed of approximately 95 % type I collagen and the remaining 5 % type III collagen (37).
Type I collagen assembles in a step-by-step hierarchical manner, from the formation of the triple helix to the aggregation of fibril into fibers. The mature, assembled fibers are essential for tissue structure, mechanics, cellular interactions, and other functions *in vivo*.
Type I collagen is extensively researched for a wide range of biomedical applications. It's a key component of tissue engineering scaffolds, and *in vitro* cell substrates for studying cell adhesion, migration, and differentiation (38).

1.8 Project aim

This project aims to explore how physical stress, imposed through varying extracellular matrix densities, affects the growth of pancreatic cancer cells.

Practically, this study involves culturing pancreatic cancer cells within different concentrations of alginate and bovine collagen. These biomaterials are chosen for their ability to mimic the stiffness and density of natural ECM found *in* v*ivo.* By adjusting the concentrations of these matrices, the project seeks to simulate various levels of physical stress and observe the resultant effect on cellular growth.

This thesis will detail the experimental design, methods, and analytical techniques employed to assess changes in cell growth.

2 Materials and Methods

2.1 Materials

2.1.1 Pancreatic Cancer Cell Lines

Pancreatic cell line used in this study are from American Type Culture Collection (ATCC) listed below in table 2-1.

Table 2-1: Cell line used in experiments.

Cell line	ATCC	Source	Morphology
PANC-1	CRL-1469	57-year-old Caucasian Male	Epithelial

2.1.2 Reagents

Reagents used in cell cultivation and experiments are listed below in table 2-2.

Table 2-2: Reagents used in experiments and cell cultivation.

Reagents	Manufacturer	Catalog No.	Use
Telocol-10 (20 ml) Type I Bovine Collagen Solution 10,2 mg/ml	Advanced Biomatrix	5226-20ML	Cell Culture

Dulbecco´s Modification of Eagles Medium (DMEM) (500 ml) With 1g/L glucose, L-glutamine & sodium pyruvate	Corning	17-207-CV	Cell Culture
Phosphate buffered saline 1X (PBS) (500 ml)	VWR	392-0442	Cell Culture
Pen-strep	Biowest	L0022-020	Cell Culture
Trypsin	Corning	25-053-Cl	Cell Culture
Fetal bovine Serum (FBS) (500 ml) Heat Inactivated	Biowest	S181H-500	Cell Culture
Muse count & Viability Kit	Luminex Corporation	637365	Cell Count and Viability
Resazurin 484 μM	Merck Life science AS	199303	Cell Count and Viability
Calcium Sulfate dihydrate	Sigma-Aldrich	31221	Alginate crosslinking
EDC	Sigma-Aldrich		Alginate crosslinking
AAD			Alginate crosslinking
Alginate HMW	FMC BioPolymer		Alginate gel
Alginate LMW	FMC BioPolymer		Alginate gel
Alginate Purified	NovaMatrix		3 D Cell Culturing

2.1.3 Prepared Solutions

Outlined below are the details of experimental solutions that was made for this project.

2.1.3.1 Complete Culture Media

Complete culture media was prepared using sterile technique with Dulbeccos Modification of Eagles Medium (DMEM) (1 g/L glucose, L-glutamie & sodium pyruvate), 1 % pen-strep, and 10 % Fetal Bovine Serum (FBS).

2.1.3.2 Resazurin

4,86 mg gram of powder was accurately weighed and mixed with sterile 40 ml Phosphate buffered saline (PBS), the solution was then filtered (0,25 µm) to make sure it was sterile. Final concentration resazurin was 484 µM. Bottle covered with aluminum foil to prevent exposure to light, stored at 4 °C in fridge.

2.1.3.3 Concentrations of Telocol-10 Type 1 Collagen Bovine Serum

Collagen concentrations were respectively prepared at 1 mg/ml and 3 mg/ml for cell culturing. Telocol-10 at 10 mg/ml was diluted using complete DMEM. All procedures were performed aseptically to prevent contamination, and collagen was kept on ice to prevent premature gelation due to its temperature sensitivity. Another measure to prevent early gelation was monitoring pH using phenol red and pH paper. If the pH was too, it could be adjusted to 7,2-7,6 using sterile NaOH.

2.1.3.4 Alginate

Alginate solutions, both non-sterile and unpurified, were formulated in concentrations of 1 % and 2 %, utilizing variants with high and low molecular wrights. For the preparation of the 1 % alginate solution, a quantity of 1 gram of alginate was accurately measured and subsequently dissolved in 99 ml of water. For the preparation of 2 % alginate solution, 2 grams of alginate was used and 98 ml of water. The mixtures were made in glass beakers, into which a magnet stir bar was introduced. The setup was positioned on a magnetic stirrer to ensure thorough mixing, where it was covered with parafilm and left to stir until the following day. Stored in fridge at 4 °C.

2.1.3.5 Calcium Sulfate

Calcium sulfate was weighed out to 4,2 grams. Then transferred to a biosafety cabinet where 20 ml of sterile water was added. The solution was mixed well and vortexed, stored in room temperature.

2.1.3.6 EDC N-(3-Dimethylaminopropyl)-N`-ethyl carbodiimide-hydro-chloride

The EDC powder must be taken from the freezer and allowed to reach room temperature. Weight out 40 mg of EDC on an analytical balance, the transferred to an Eppendorf tube and mixed with 400 µl of MES buffer.

2.1.3.7 Purified and Sterile Alginate Solution

The purified alginate was sterilized by autoclaving. A 1 % and 2 % sterile alginate solution was prepared under sterile conditions within a biosafety cabinet, by weighing 0.1 and 0,2 grams on an analytical balance, which then was transferred to sterile glass bottles and mixed with 9,9 and 9,8 ml of complete DMEM. A sterile magnetic stir bar was placed into the bottle before it was securely sealed with a tight cap. The bottles were then placed on a magnetic stirrer and left to mix until the subsequent day. Stored in fridge at 4 °C.

2.1.3.8 Rotenone

Rotenone was diluted from a concentration of 50 µM to 100 nM and used for treating cells cultured in collagen.

2.1.4 Consumables

Consumables and other equipment used in the experiments are listed below in table 2-3.

Table 2-3: Items used during experiments.

Consumables	**Manufacturer**	**Catalog No.**	**Use**
T-75 Flasks	Corning	734-0050	Cell Culture
10 ml serological pipette	VWR	612-3700	Cell Culture
2 ml serological pipette for aspiration	Greiner	GREI710183_1000	Cell Culture
5 ml serological pipette	VWR	612-3702	Cell Culture
1 ml syringe	Braun	9161406V	3 D Cell Culture
3 ml syringe with luer-lok	BD Medical	14-823-435	3 D Cell Culture
96 Wells-F, Surface Treated	VWR	10062-900	3 D Cell Culture

2.1.5 Instruments

The main instruments utilized in the various experiments are listed below in Table 2-4.

Table 2-4: Instruments used in experiments.

Instruments	Manufacturer	Use
Muse Cell Analyzer	EMD Millipore Corporation	Cell Count & Viability
Spectramax Paradigm Multi-Mode Microplate Reader	Molecular Devices, Inc. SER 33 270-1108	Cell count & Viability
Kubota 2800 Sentrifuge		Pelleting
Rheometer	Ta Instruments	Measuring Viscoelasticity

2.2 Methods

All work involving cell lines in this project was carried out in the biosafety level 2 cell culture laboratories at Måltidets Hus, utilizing aseptic technique within a laminar flow cabinet. The rheological properties of Alginate were examined using a rheometer at Nofimas laboratory, which facilitated these assessments.

2.2.1 Aseptic Technique

During this study, strict aseptic techniques were meticulously employed for all the cell culture procedures within a laminar flow cabinet. Such measures were imperative to prevent contamination by fungi, bacteria, or inadvertent cross contamination with alternate cell cultures. Consistent with best practices, personal protective equipment-including laboratory coats and gloves were always used during experimentation.

All non-sterile equipment was sanitized using autoclaving or washing with 70 % ethanol prior to application. The laminar flow workbench was always cleaned with ethanol both pre-and post-operations to ensure a sterile environment. Following each session, ultraviolet light sterilization was enacted to eradicate any residual microbial presence, supplementing the

mechanical sanitation process. The cabinet has filters and internal fans that control airflow and capture particles, thereby reducing the chance of contamination.

2.2.2 Cell Culture Initiation

Panc-1 cells were retrieved from the cryotank and gently thawed at 37 °C. The cells were transferred to a surface treated T-75 flask, and supplemented with complete DMEM, after which the flask was placed in an incubator at 37 °C with CO_2 concentration of 5 %. CO_2 plays a crucial role in maintaining the pH of the culture medium, serving as a buffering agent. Over the following two days, the medium was changed using a sterile pipette to aspirate the old media, and 10 ml of fresh complete DMEM media was added.

2.2.3 Cell Passaging

Due to rapid proliferation and high cell density, splitting of the cell culture was necessary approximately twice a week. The cells were split at 1:5 ratio by first aspirating the old medium using a 2 ml aspiration pipette, then rinsing with PBS, The PBS wash is crucial for removing trypsin inhibitors present in the medium. To detach the cells from the flask, trypsin was used. Figure 2-1 illustrating how the cells look before they are trypsinized. The cells underwent trypsinization by the addition of 2 ml of 0,25 % trypsin-EDTA and were then incubated for 2 minutes. This step speeds up the process as trypsin's proteolytical activity is enhanced at the physiological temperature of 37 °C, which is ideal for the digestion of proteins in cell culture. Microscopic examination revealed the expected rounding of the cells, Figure 2-2, indicating effective trypsinization. Following this, 3 ml of complete DMEM was added to the cell suspension and gently mixed up and down with a 10 ml serological pipette. In this reaction, the alpha-1 antitrypsin in FBS binds to trypsin, inhibiting its protease activity and stopping trypsinization (39). Afterward, 4 ml of the solution was aspirated from the flask and appropriately discarded. 10 ml of complete DMEM were added to the remaining 1 ml of cell suspension. The flask was then returned to the incubator to continue the culture process.

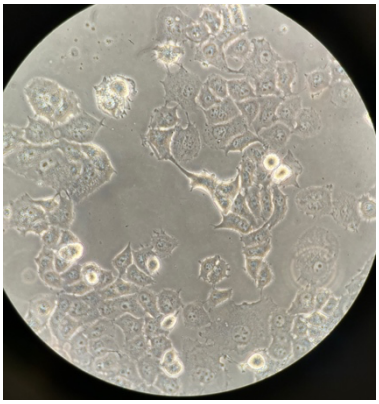

Figure 2-2: Microscopic picture showing high cell density before cells are trypsinized.

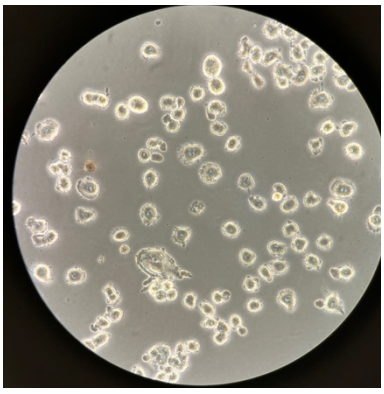

Figure 2-1: Microscopic examination shows rounding of cells after trypsinization.

2.2.4 Cultivating Panc-1 in Collagen and Alginate Matrices

2.2.4.1 Cells Cultured in Collagen

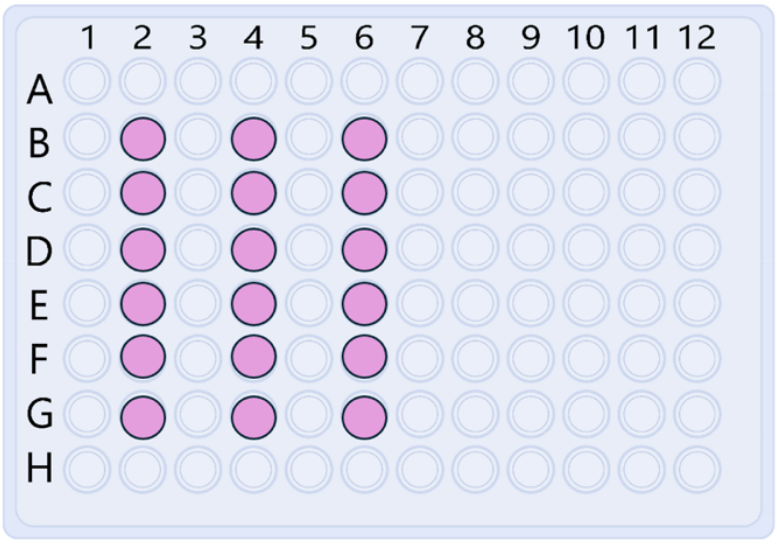

Figure 2-3: Illustration of 96 well plate with collagen matrices. 1 mg/ml collagen in well 2B-G. 3 mg/ml collagen in well 4B-G. Control of 1 mg/ml collagen in 6B-6D, and final control of 3 mg/ml in well 6E-G (40).

In this study, a 96-well plate was utilized to culture cells at two distinct concentrations: 5000 and 10000 cells per well in respective concentrations of 1 mg/ml and 3 mg/ml of collagen, shown in Figure 2-3. Throughout this procedure, both the medium and collagen were meticulously maintained on ice to prevent premature gelation of the collagen. The cell suspension and collagen were carefully diluted with the medium to achieve the correct concentrations, taking care to avoid the introduction of air bubbles into the solution. 100 µl of the cell-collagen mixture was pipetted into the wells on the plate, while PBS was pipetted into the surrounding wells to avoid dehydration. The plate was subsequently incubated for one hour to allow for gelation. After this period, an additional 100 µl of complete DMEM was added to each well to nourish the cells and prevent the gel from dehydrating. The plate was incubated for a period of 3-4 days at 37 degrees Celsius with a CO_2 concentration of 5 %. Following incubation, a resazurin assay was introduced to the wells to assess cell viability through fluorescence measurements. The instrument settings were adjusted to an excitation wavelength of 530-570 nm.

2.2.4.2 Cells Cultured in Alginate

In this study, concentration of 1 % and 2 % purified alginate medium was employed. The experimental setup included a 96-well plate, with each well containing 100 µl and 10,000 cells per 100 µl. Cell counting was performed with a Muse analyzer, and the cells were

diluted to the concentration needed. Following centrifugation to pellet the cells, the supernatant was meticulously aspirated, and the cell pellet was resuspended in sterile alginate medium. To ensure a bubble-free transfer of the alginate-cell mixture into luer-lok syringes, a careful method was used.

Figure 2-4: Illustration of a luer-lok syringe with connector attached.

First, a 3 ml syringe equipped with a luer-lok connector was taken, illustration of equipment in Figure 2-4.

Instead of drawing the mixture directly with the syringe, which could easily introduce air bubbles, a 1000 µl pipette, which offers more control, was used to draw up the mixture, shown in Figure 2-5. This pipette was then positioned against the opening of the syringe. By gently pulling on the syringe's plunger, the alginate-cell mixture was coaxed into the syringe from the pipette.

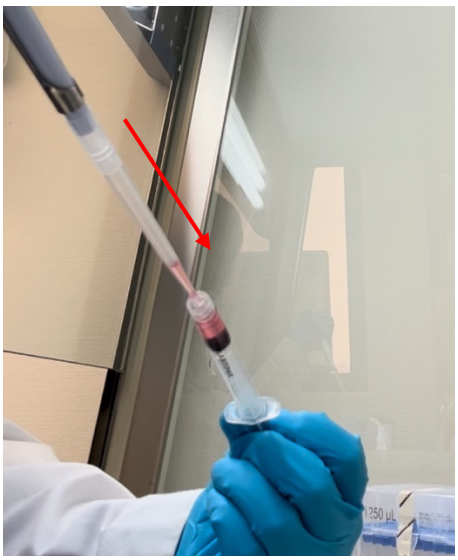

Figure 2-5: Illustration of method to avoid air bubbles. The pipette with alginate-cell mixture positioned against opening of syringe. by gently pulling the syringe plunger, the alginate-cell mixture was coaxed into the syringe.

Doing this slowly and steadily helped to ensure that the mixture entered the syringe without trapping any air. Subsequently the alginate-cell mixture underwent ionic crosslinking before loaded into 1 ml syringes. It was critical to confirm a secure, airtight seal on the syringes. A small amount of the alginate-cell solution was gently expelled up to the tip to create a continuous phase up to the opening of the 3 ml syringe, onto which the 1 ml syringe was subsequently attached, effectively preventing the incorporation of air bubbles. Approximately 100 µl of the solution was dispersed into wells on the plate using a 1 ml syringe, with the volume being estimated by eye. To mitigate evaporation, sterile PBS was added to the empty peripheral wells, and an additional 100 µl of fresh medium was layered over the gels to maintain nutrient availability and hydration. The plate was then incubated at 37 degrees Celsius for 48-72 hours with a CO_2 concentration of 5 %. Following incubation, a resazurin assay was introduced to the wells to assess cell viability through fluorescence measurements. The instrument settings were adjusted to an excitation wavelength of 530-570 nm.

2.2.5 Resazurin Cell Viability Assay

Resazurin assay utilize the reduction of an oxidized blue dye to a pink, fluorescent product, resorufin, by living cells. While florescence monitoring is the primary method for observing this reaction due to its high sensitivity, absorbance measurements can also be used, albeit with a slight decrease in sensitivity (41).

Upon introducing resazurin to a cell culture, the dye solution is reduced to resorufin by metabolically active cells, this change is quantifiable with analytical instruments. Initially, a resazurin stock solution was formulated at 484 µM, which was then diluted to a working concentration of 44 µM using complete DMEM. Each well of a 96-well plate, which contained a predefined arrangement of cells and collagen, was loaded with 100 µl of the resazurin solution. The plate underwent a subsequent incubation for four hours to facilitate the reduction of resazurin to resorufin. Post-incubation, the resazurin was aspirated with care from each well and transferred to new wells for spectroscopic analysis. Measured fluorescence was done with excitation wavelength at 530-560 nm, and absorbance filter was set to 570-600nm using the Spectramax Paradigm Multi-Mode Microplate Reader.

2.2.6 Crosslinking Methodology

2.2.6.1 Ionic Crosslinking Methodology

The process of ionic crosslinking of alginate utilizes calcium sulfate as the crosslinking agent. In this study, to fabricate test gels for rheology measurements, formulations comprising 9 ml of alginate solution and 360 µl of calcium sulfate were prepared. Figure 2-6, utilizing syringes equipped with luer-lok connectors, 9 ml of the alginate solution was carefully drawn into one syringe, with meticulous efforts made to eliminate all air bubbles. Similarly, a luer-lok syringe was filles with 360 µl of calcium sulfate solution, ensuring the removal of air bubbles to prevent any potential mixing inconsistencies. The two syringes were then securely connected via a luer-lok connector. Subsequently to connection, the alginate and calcium sulfate solutions were rapidly and thoroughly mixed by energetically moving the syringe plungers back and forth several times, facilitating the ionic crosslinking reaction. The crosslinked alginate was then extruded onto a glass slide prepared with 1 mm microscope slides placed strategically at the corners, serving as spacers. A second glass slide was carefully positioned on top to standardize the gel thickness, ensuring uniform gel heights (42).

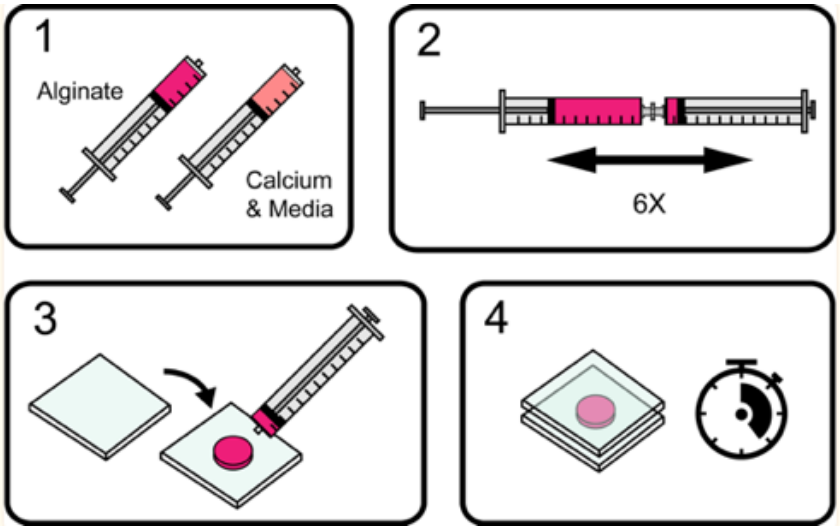

Figure 2-6: Summary of the basic steps for ionically crosslinked alginate hydrogel preparation: Alginate is swiftly combined with calcium and media, initiating a rapid gelation process that results in the formation of a three-dimensional polymeric matrix (42).

2.2.6.2 Covalent Crosslinking Methodology

In the preparation of covalent crosslinkers for alginate, it is essential to prepare a fresh EDC mixture for each reaction. 300 ml of the EDC mixture were transferred into a luer-lok syringe, in parallel, another syringe was filled with 300 ml of AAD solution. A luer-lok syringe with 3

ml of alginate was prepared. Crosslinking was initiated by first mixing the alginate and AAD solutions using a connector. Covalent crosslinking reaction is completed by combining alginate solution with EDC mixture, by again utilizing a connector between the syringes. Solutions were rapidly and thoroughly mixed by energetically moving the syringe plungers back and forth several times. The covalently crosslinked alginate was then extruded onto a 6 well plate and placed in fridge overnight to gel (42).

2.3 Measuring Mechanical Properties of Alginate

The mechanical properties of alginate were measured using a rheometer at the Nofima laboratory. This was done to find the viscoelasticity of the alginate gels. The gels examined contained alginate concentrations of 1% and 2%, with 5 replicates of each concentration. Gels with a height of 1 mm and 20 mm were cut out using a metal plunger to fit a 20 mm diameter geometry.

Instrumental settings:

- Gap 700 µm
- Frequency 1,0 Hz
- Temperature 37 ° C
- Oscillation Frequency 1,0 %
- Strain 0,1 % - 400,0 %

The data were analyzed by conducting regression analyses on each individual replicate, after which the average elasticity values were computed. To create linear regression lines, it was necessary to first generate a stress-strain plot, with strain on the x-axis and stress on the y-axis. This process was carried out to identify the linear region of the plot. Once this region was determined, the corresponding values were selected for a new plot. This subsequent plot was then used to create a scatter plot with a trendline, enabling a more detailed analysis of the data.

3 Results

3.1 Cell Viability in the Cell Line Panc-1

A resazurin viability assay was conducted in two experiments on Panc-1 cells cultured in 96-well plates for 48 hours, measured fluorescence using resazurin with instrument settings adjusted to excitation wavelength of 530-570 nm.

Results shown in Figures 3-1, and 3-2 show that viability levels trailed off from cell concentration of 15000 to 20000, indicating a saturation point beyond which further changes in cell viability are not accurately measured, this finding establishes an upper limit for subsequent experimentation.

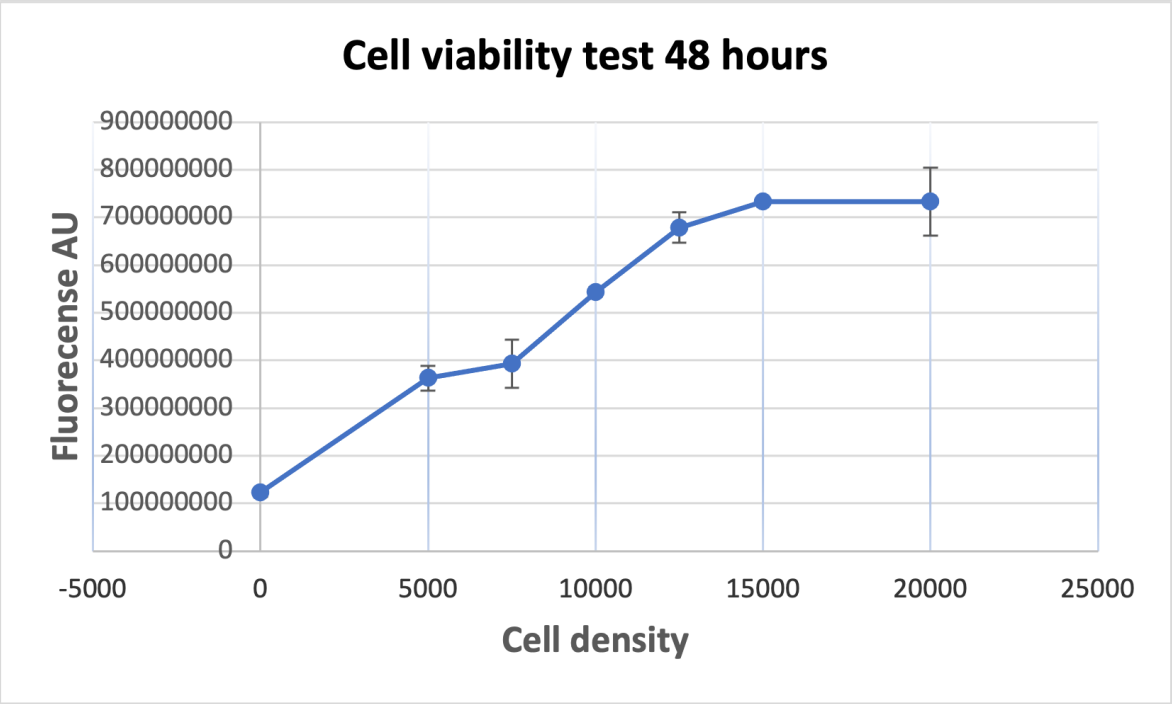

Figure 3-1: Resazurin viability assay performed on Panc-1 cells, the graph levels out between cell concentrations of 15000 and 20000 indicating a saturation point.

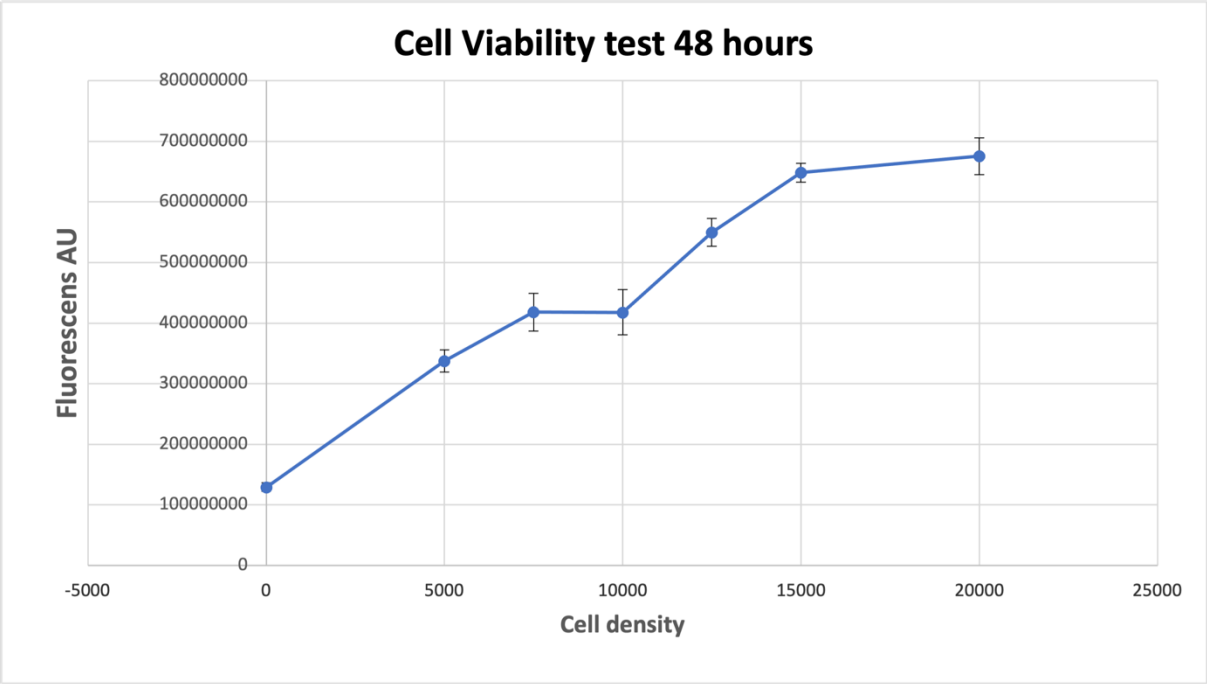

Figure 3-2: Resazurin viability assay performed on Panc-1 cells was repeated a second time and yielded similar results as the first experiment. Results show that the graph levels out between cell concentrations of 15000 and 20000.

3.2 3 D Culturing in Collagen

To investigate if physical stress affects pancreatic cancer cell proliferation, the PANC-1 cells were cultured within a collagen matrix at 1 mg/ml and 3 mg/ml concentrations. The duration of the experiments ranged from 48 hours to 96 hours. Fluorescence was measured to compare cell viability in the different concentrations using resazurin assay with instrument settings adjusted to excitation wavelength of 530-570 nm.

The cells were cultured on 96-well plates with cell concentrations of 5000 and 10000 per well, included a control for both collagen concentrations on each plate.

Averages and standard deviations were calculated for all groups. The outlier calculator from GraphPad, with a significance level of 0,05 was also applied to all data to check for potential outliers that could be excluded (43). Outliers excluded are marked with red color and presented in tables in appendix. Control values were subtracted from the data presented in all the graphs, and error bars represent standard deviations.

3.2.1 PANC-1 PROLIFERATION IN 1 AND 3 MG/ML COLLAGEN OVER 48 HOURS

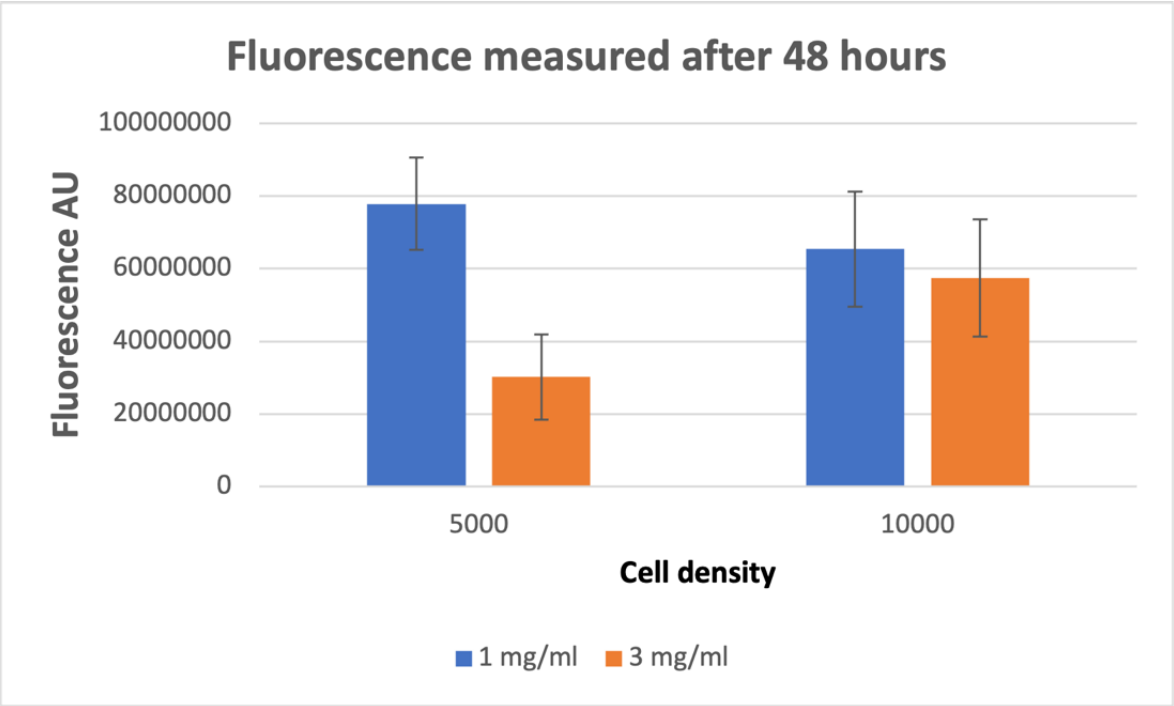

Figure 3-3: Fluorescence measurements from cells cultured in 1 mg/ml and 3 mg/ml collagen concentration over a two-day incubation period. This figure presents data from two independent replicates with cell densities of 5000 and 10000 per well, indicating higher proliferation in the 1 mg/ml concentration. Error bars represent standard deviations.

Cells were cultured in a collagen matrix for a two-day incubation period. Two independent replicates of the experiment were conducted on separate days, each involving cell concentrations of 5000 and 10000 cells per well, cultured in collagen concentrations of 1 mg/ml and 3 mg/ml. Controls were included for both collagen concentrations in each replicate and fluorescence was measured using a resazurin assay. The mean control value was subtracted from the mean fluorescence measurements, and standard deviation was used for the error bars.

Measured fluorescence, as shown in Figure 3-3, indicates that cell concentrations of 5,000 and 10,000 within a 1 mg/ml collagen matrix exhibit higher proliferation compared to the 3 mg/ml matrix.

3.2.2 PANC-1 PROLIFERATION IN 1 AND 3 MG/ML COLLAGEN OVER 72 HOURS

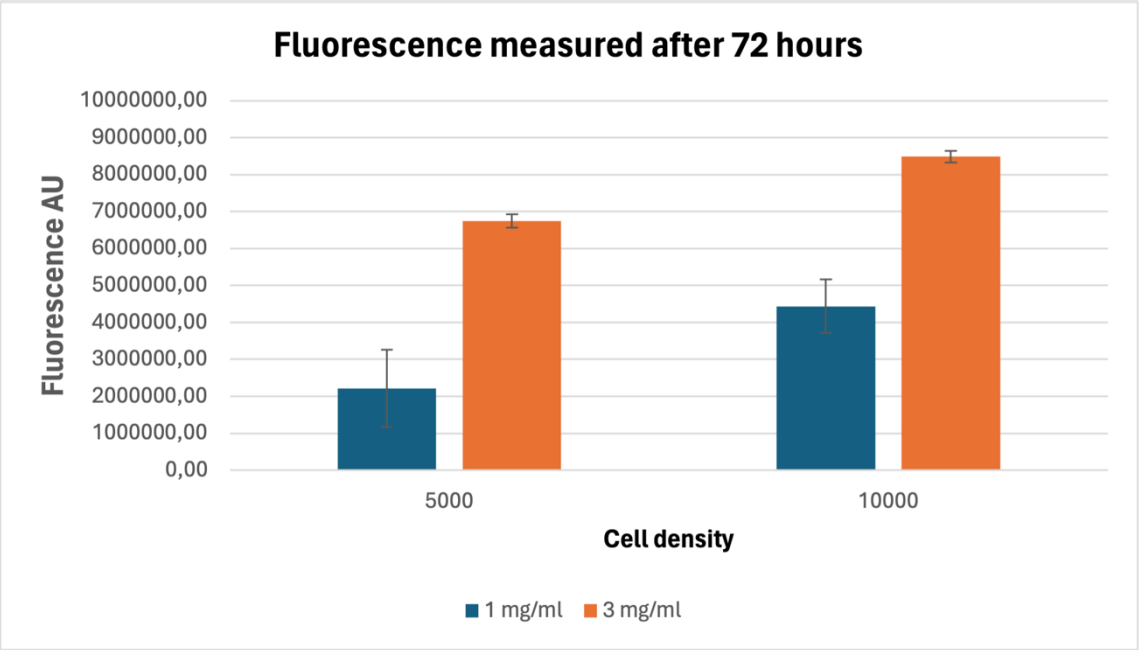

Figure 3-4: This figure presents data from two independent replicates with cell densities of 5000 and 10000 per well. Measured fluorescence show higher proliferation in cell densities of 5000 and 10000 cells per well in concentration of 3 mg/ ml collagen. Control values have been subtracted and error bars represent standard deviations.

Cells were cultured in a collagen matrix for a three-day incubation period. Two independent replicates of the experiment were conducted on separate days, each involving cell concentrations of 5000 and 10000 cells per well, cultured in collagen concentrations of 1 mg/ml and 3 mg/ml. Controls were included for both collagen concentrations in each replicate and fluorescence was measured using a resazurin assay. The mean control value was subtracted from the mean fluorescence measurements, and standard deviation was used for the error bars. However, the background control value was much higher in the 1 mg/ml compared to 3 mg/ml (11481359 for 1 mg/ml and 9182750 for 3 mg/ml), this has influenced the values presented in the columns of the graph, marked red in Table 3-1.

Results in Figure 3-4 shows that the measured fluorescence indicates higher proliferation within both replicates in 3 mg/ml collagen concentration compared to the 1 mg/ml concentration.

Table 3-1: The background control value in measured fluorescence (marked in red) was much higher in the 1 mg/ml compared to 3 mg/ml. This has influenced the fluorescence values for the replicates in 1 mg/ml collagen presented in the columns of the graph in Figure 3-4.

Concentration	Number of cells	Mean value	Standard deviation
1 mg/ml	0	11481359,5	230210,6
	5000	13696425,3	1274529,1
	10000	15918435,7	954283,7
3 mg/ml	0	9182750,5	796099,7
	5000	15923144,3	974553,9
	10000	17669492,7	955469,4

3.2.3 PANC-1 PROLIFERATION IN 1 AND 3 MG/ML COLLAGEN OVER 96 HOURS

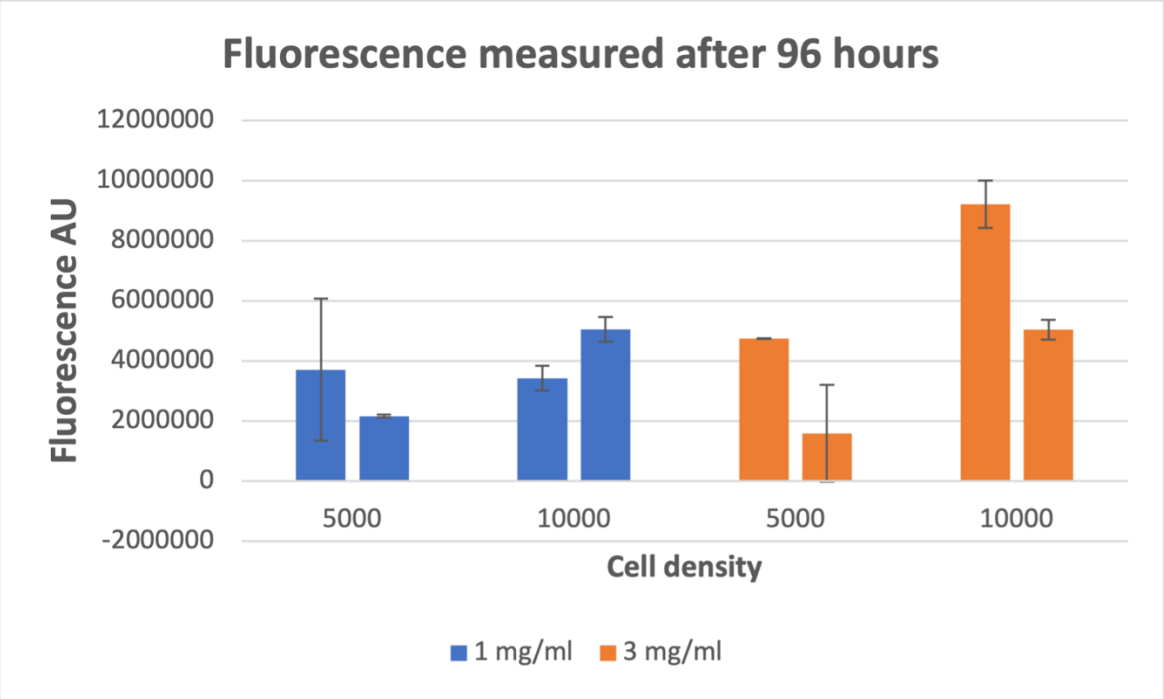

Figure 3-5: This figure presents data from two identical experiments, comprising of a total of eight replicates with cell densities of 5000, and 10000 per well. Fluorescence was measured using a resazurin assay. Standard deviation was used for the error bars. The results illustrated in the figure show a high standard deviation in two replicates of 5000 cells in 3 mg/ml collagen and 1 mg/ml. There is no difference observed in proliferation of the two replicates of 10000 cells, a higher viability for 10000 cells cultured in 3 mg/ml compared to 1 mg/ml.

In Figure 3-5 results from two identical experiments are shown, comprising of a total of eight replicates. Of these, four replicates involved culturing 5000 cells per well in 1 mg/ml collagen, while the remaining four replicates involved 10000 cells per well cultured in 3 mg/ml collagen. Controls were included for all replicates across both collagen concentrations

but subtracted from values presented in the graph. Fluorescence was measured using resazurin assay with instrument settings adjusted to excitation wavelength of 530-570 nm. Standard deviation was used for the error bars.

The results illustrated in the figure show a high standard deviation in two replicates of 5000 cells in 3 mg/ml collagen and 1 mg/ml, these results can be excluded. The results in the graph indicate higher proliferation in 3 mg/ml collagen compared to the 1 mg/ml concentration.

3.2.4 3 D PANC-1 Treated with Rotenone

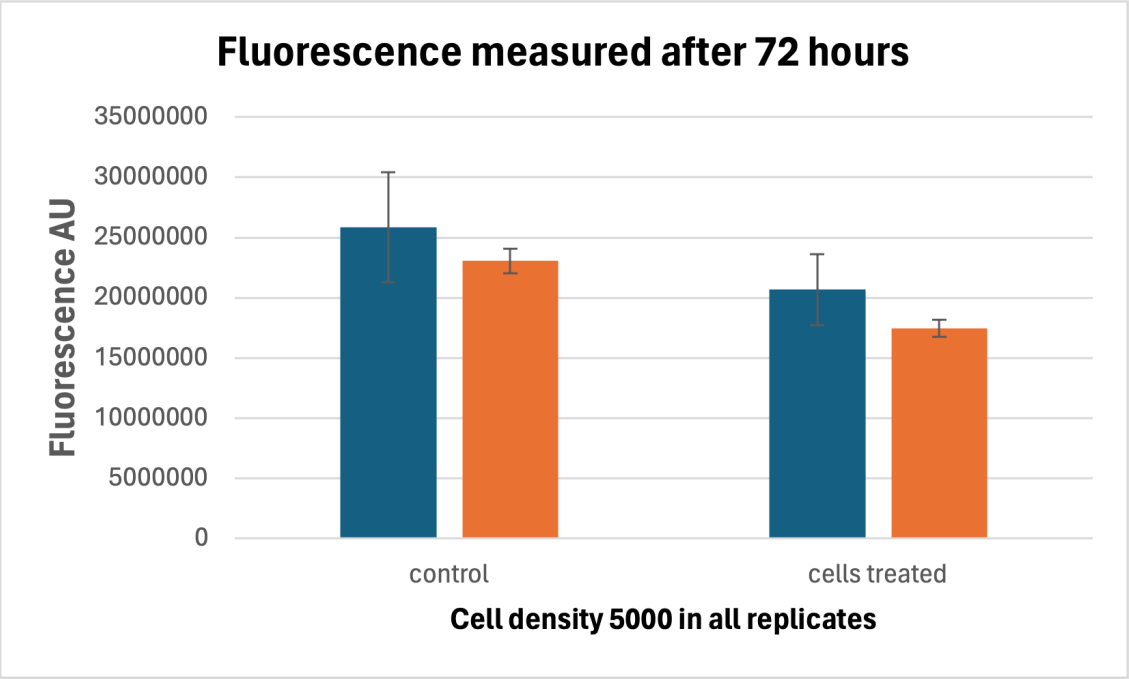

Figure 3-6: Panc-1 cells were cultured in a collagen matrix for a three-day incubation period and treated with 100 nM rotenone. All replicates containing concentrations of 5000 cells per well, cultured in collagen concentrations of 1 mg/ml (blue columns) and 3 mg/ml (orange columns) measured viability was higher in the control group than in the treated group. Viability was somewhat higher in the 1 mg/ml collagen concentration. It can also be observed that viability in the treated cells was greater in the 1 mg/ml concentration compared to the 3 mg/ml.

Panc-1 cells were cultured in a collagen matrix for a three-day incubation period and treated with 100 µl of a 100 nM rotenone concentration. All replicates containing concentrations of 5000 cells per well, cultured in collagen concentrations of 1 mg/ml (blue columns) and 3 mg/ml (orange columns). Controls were included for both collagen concentrations in each replicate and fluorescence was measured using a resazurin assay. The mean control value was

subtracted from the mean fluorescence measurements, and standard deviation was used for the error bars.

Measured fluorescence shown in Figure 3-6 show that proliferation was higher in the control group than in the treated group, although proliferation was somewhat higher in the 1 mg/ml collagen concentration, but the standard deviation is also higher here, compared to the replicates in 3 mg/ml concentration. It was also observed that proliferation in the treated cells was greater in the 1 mg/ml concentration compared to the 3 mg/ml.

3.3 3D Culturing in Alginate

To investigate if physical stress affects pancreatic cancer cell proliferation, the PANC-1 cells were cultured within an alginate matrix at 1 % and 2% concentrations. The duration of the experiments ranged from 24 hours to 72 hours. Fluorescence was measured to compare cell viability in the different concentrations using resazurin assay with instrument settings adjusted to excitation wavelength of 530-570 nm.

The cells were cultured on 96-well plates with cell concentrations 10000 per well and a control on each plate.

Averages and standard deviations were calculated for all groups. The outlier calculator from GraphPad, with a significance level of 0,05 was also applied to all data to check for potential outliers that could be excluded (43). Control values were subtracted from the data presented in the all the graphs, and error bars represent standard deviations.

3.3.1 Panc-1 Cultured in 1 % Alginate 48 Hours

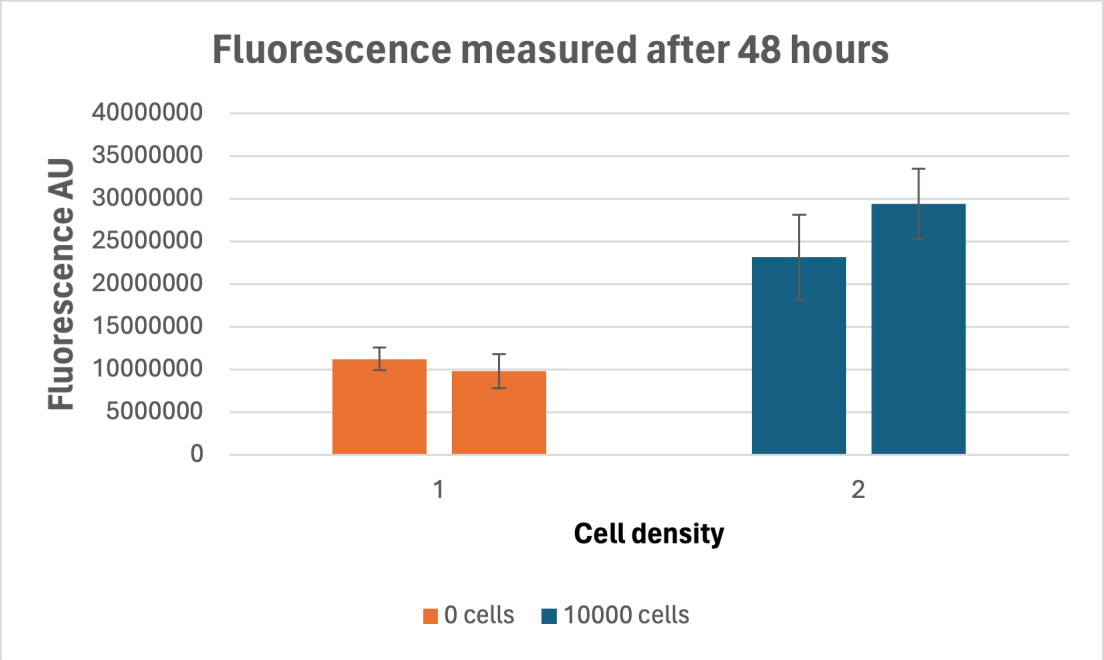

Figure 3-7: This figure presents data from two independent replicates with cell densities of 10000 per well cultured in 1 % alginate for a two-day period. The mean control value was subtracted from the mean fluorescence measurements, and standard deviation was used for the error bars. Results show little difference in proliferation across the two replicates of 10000 cells.

Panc-1 cells were cultured in an alginate matrix for a two-day incubation period. Replicates with a concentration of 10000 cells per well was grown in 1 % alginate concentration. Controls were included for in each replicate and fluorescence was measured using resazurin assay with instrument settings adjusted to excitation wavelength of 530-570 nm. The mean control value was subtracted from the mean fluorescence measurements, and standard deviation was used for the error bars. Results shown in Figure 3-7 shows little difference in proliferation across the two replicates of 10000 cells.

3.3.2 Panc-1 Cultured in 1 % and 2% Alginate for 24 Hours

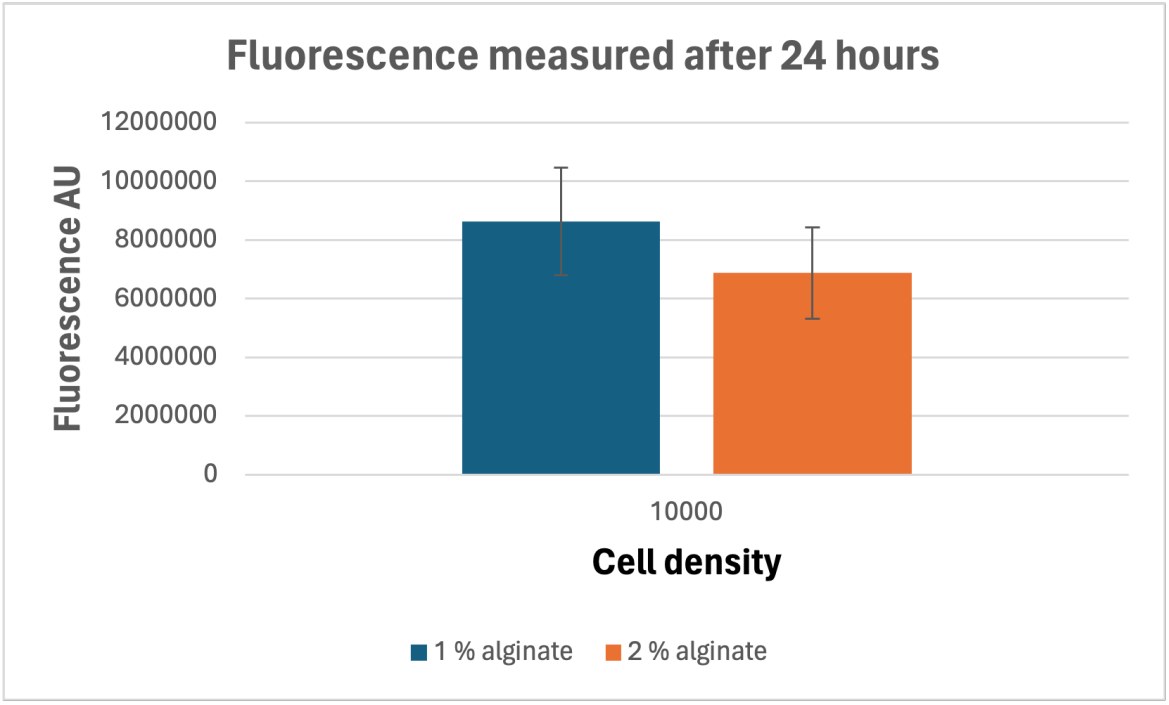

Figure 3-8: This figure presents data from Panc-1 cells replicates with cell densities of 10000 per well cultured in 1 % and 2 % alginate for 24 hours. The mean control value was subtracted from the mean fluorescence measurements, and standard deviation was used for the error bars. Results show higher proliferation in the 1 % concentration compared to 2 % alginate.

Panc-1 cells were cultured in an alginate matrix for a 24-hour incubation period. Replicates with a concentration of 10000 cells per well was grown in 1 % and 2 % alginate concentration. Controls were included for in each replicate and fluorescence was measured using resazurin assay with instrument settings adjusted to excitation wavelength of 530-570 nm. The mean control value was subtracted from the mean fluorescence measurements, and standard deviation was used for the error bars. Results shown in Figure 3-8 showed higher cell proliferation in 1 % alginate compared to 2 %.

3.3.3 Panc-1 Cultured in 1 % and 2% Alginate for 48 Hours

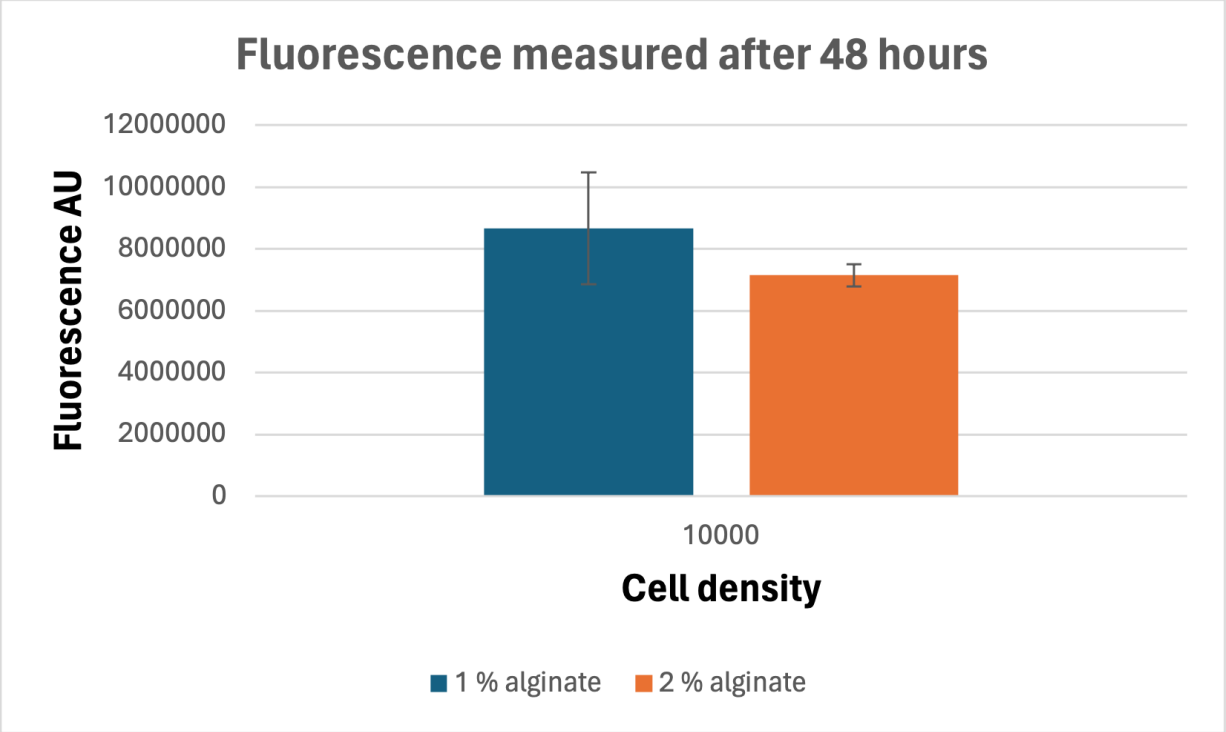

Figure 3-9: This Figure presents data from Panc-1 cells replicates with cell densities of 10000 per well cultured in 1 % and 2 % alginate for a two-day period. The mean control value was subtracted from the mean fluorescence measurements, and standard deviation was used for the error bars. Results show higher cell proliferation in the 1 % concentration compared to 2 % alginate.

Panc-1 cells were cultured in an alginate matrix for a 48-hour incubation period. Replicates with a concentration of 10000 cells per well was grown in 1 % and 2 % alginate concentration. Controls were included for in each replicate and fluorescence was measured using resazurin assay with instrument settings adjusted to excitation wavelength of 530-570 nm. The mean control value was subtracted from the mean fluorescence measurements, and standard deviation was used for the error bars.

Results shown in Figure 3-9 shows higher cell proliferation in the 1 % concentration compared to the 2 % concentration of alginate.

3.3.4 Panc-1 Cultured in 1 % and 2% Alginate for 72 Hours

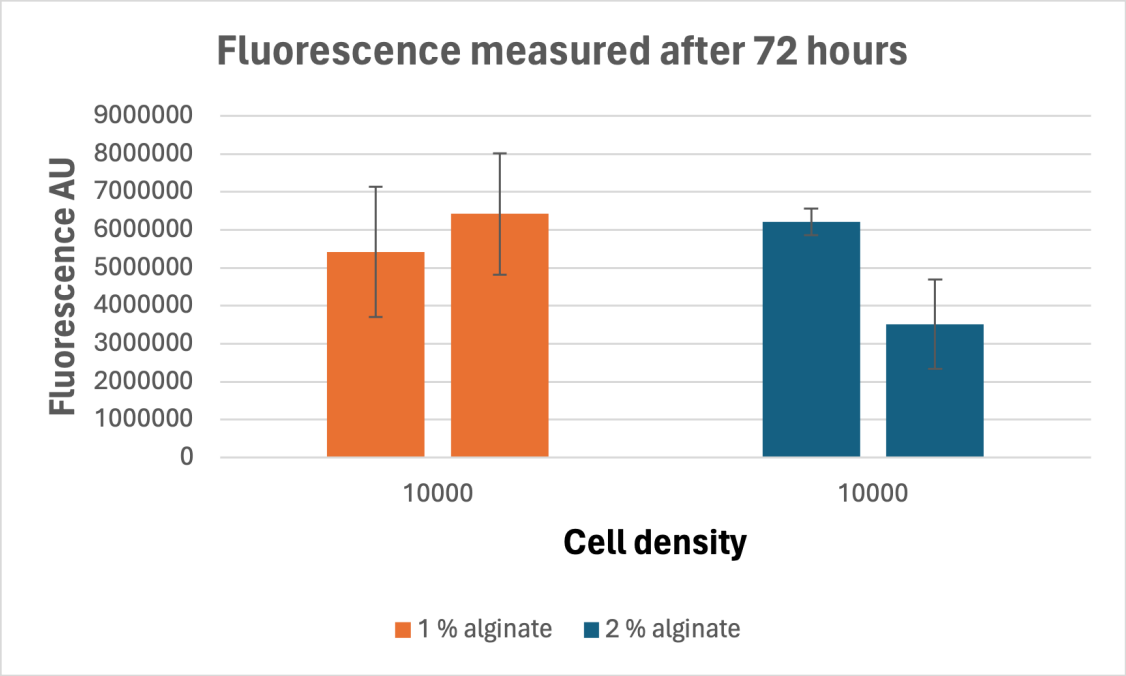

Figure 3-10: This figure presents data from Panc-1 cells replicates with cell densities of 10000 per well cultured in 1 % and 2 % alginate for a three-day period. The mean control value was subtracted from the mean fluorescence measurements, and standard deviation was used for the error bars. Results show higher cell proliferation in the 1 % concentration compared to 2 % alginate.

Panc-1 cells were cultured in an alginate matrix for a three-day incubation period. Replicates with a concentration of 10000 cells per well was grown in 1 % and 2 % alginate concentration.

Controls were included for in each replicate and fluorescence was measured using resazurin assay with instrument settings adjusted to excitation wavelength of 530-570 nm. The mean control value was subtracted from the mean fluorescence measurements, and standard deviation was used for the error bars.

Results shown in Figure 3-10 shows that the cells have proliferated more in the 1 % concentration compared to 2 %.

3.4 Rheological Measurements of 1 % and 2 % Alginate Gels

Rheological measurements were conducted on 1% and 2 % alginate gels as these concentrations were used to culture Panc-1 cells. The results from the rheology measurements performed on alginate were the average values from five replicates of each concentration. The Figures 3-11 and 3-12 are from just one replicate and are included in this thesis to demonstrate how the elastic properties was determined. Respectively by plotting strain values

on x-axis and stress on y-axis, to identify the linear region. Whereafter the values in the linear region were used to make a new plot with trendline showing the value of viscoelasticity. The average measured elasticity in 1% alginate gel was 0.00722 kPa, whereas for 2% alginate, it was higher at 0.01186 kPa.

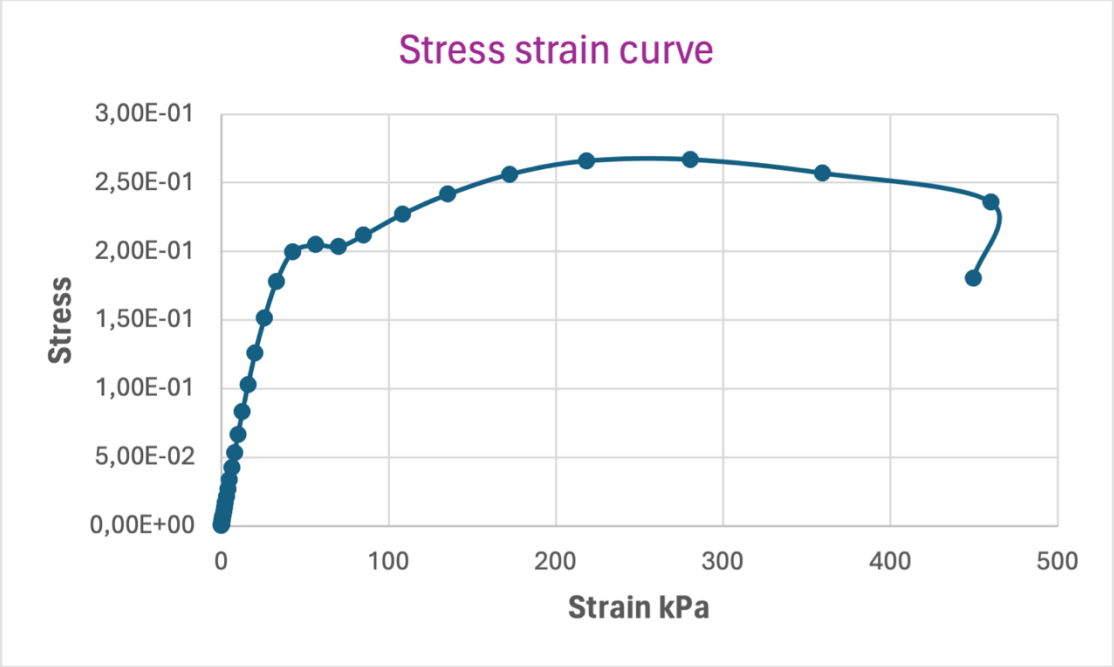

Figure 3-11: Graph present the results from one of the experimental replicates. Strain values were plotted on the x-axis, while stress values were plotted on the y-axis for all replicates. The linear region within the data was identified, allowing for the selection of appropriate data points. These points were then used to generate a new plot, where a trendline was established to analyze the relationship between stress and strain.

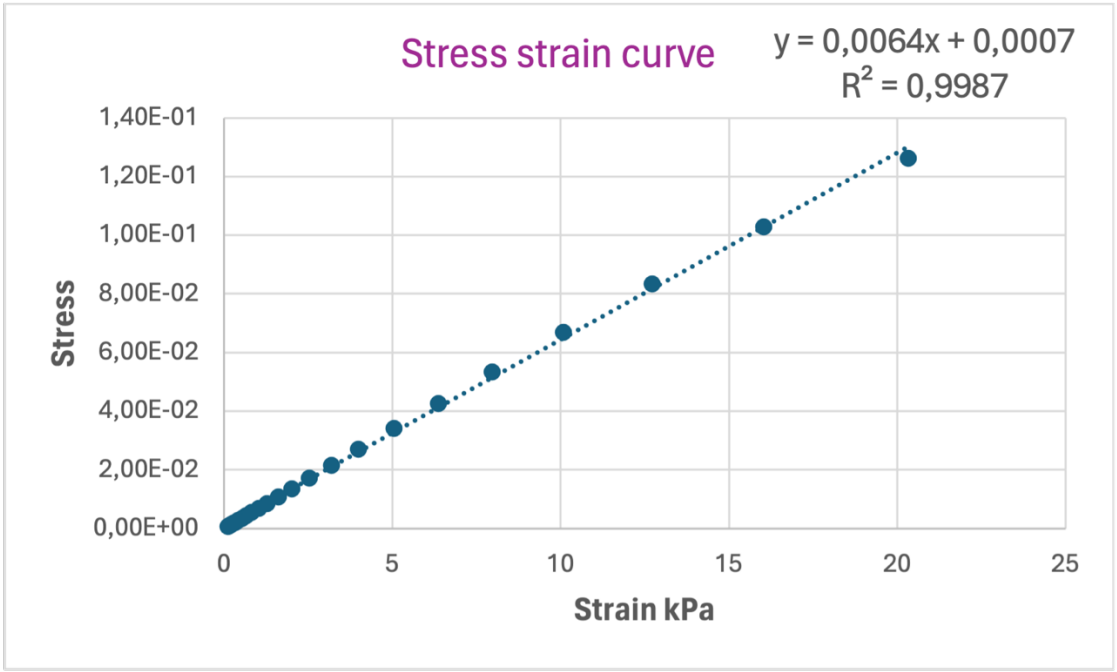

Figure 3-12: Graph presents the trendline results derived from the linear region in Figure 3-11. The data points identified within the linear region of the plot from Figure 3-11 were utilized to generate this new plot, which includes a trendline. The elastic properties of alginate measured for this replicate is 0.0064 kPa.

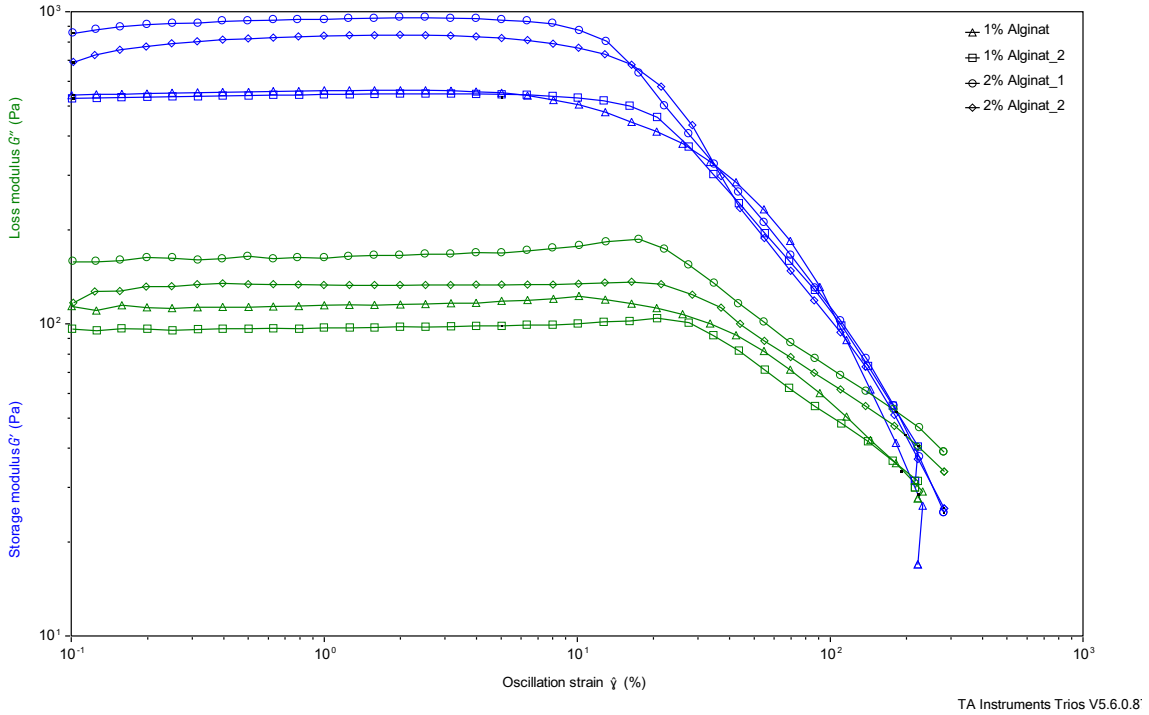

Figure 3-13 These graphs present the storage modulus (G') and loss modulus (G") across a range of oscillation strains for both 1 % and 2 % alginate concentrations. The results indicate a clear distinction in the mechanical properties between the two concentrations. The 1% alginate exabits lower G', suggesting lesser elasticity and forming a weaker gel, whereas the 2 % alginate demonstrates significantly higher G' values, indicative of greater elasticity and a more robust gel structure. Additionally, the loss modulus (G") is also higher for the 2 % alginate, reflecting increased viscosity and greater energy dissipation during deformation.

The results in Figure 3-13 figure presents the storage modulus (G') and loss modulus (G") across a range of oscillation strains for both 1% and 2% alginate concentrations. The results indicate a clear distinction in the mechanical properties between the two concentrations. The 1% alginate exhibits lower G', suggesting lesser elasticity and forming a weaker gel, whereas the 2% alginate demonstrates significantly higher G' values, indicative of greater elasticity and a more robust gel structure. Additionally, the loss modulus (G") is also higher for the 2% alginate, reflecting increased viscosity and greater energy dissipation during deformation.

4 Discussion

4.1 Methodological Considerations Using Resazurin Assay

Viability levels trailed off from cell concentration of 15000 to 2000, shown Figure 3-1 and 3-2. Identifying the linear region in the resazurin assay was important due to finding cell concentrations suitable for further experimentations. Beyond the linear range in resazurin, the assay's ability to accurately reflect changes in cell densities or viability diminishes. At high cell densities, for instance, the dye might be completely reduced before all cells have ha opportunity to interact with it. This leads an underestimation of cell numbers (44).

4.2 Collagen Density Influences Panc-1 Response to Rotenone

The measured fluorescence, as depicted in Figure 3-6 indicates that cell proliferation was higher in the control group than in the replicates treated with rotenone. Interestingly, proliferation was somewhat higher at the 1 mg/ml collagen concentration, though it was accompanied with a higher standard deviation compared to the replicates at the 3 mg/ml concentration. Additionally, treated cells exhibited greater proliferation at the 1 mg/ml concentration than the 3 mg/ml concentration. This outcome aligns with expectations considering the known effects of the compound. The inhibitors toxicity primarily stems from its ability to inhibit mitochondrial complex I. the mechanisms of inhibition likely contributed to reduced cell proliferation in the treated groups. The observed variability in proliferation rates between different collagen concentrations may be linked to how collagen density influences microenvironment, potentially affecting the cells vulnerability to mitochondrial disruption.

It is plausible that lower collagen density facilitates better nutrient and waste exchange or provides less mechanical constraint on the cells, thereby enhancing their overall viability, similar results have been found in one study. This study explored the effectiveness of collagen-nanocellulose pancreatic cancer cells in 3D culturing. They found that by adjusting stiffness of collagen this affected the cancer cells. Specifically, their finding demonstrated that cells embedded in matrices with low collagen density exhibited increased migration. As a result, cells dispersed from their original clusters, facilitating the formation of smaller structures. Conversely, they also found that high collagen densities impeded cell migration, leading to the formation of larger multicellular cluster (45).

4.3 Density in Hydrogels Impact Cancer Cell Growth

4.3.1 Collagen Density Influences Panc-1 Growth

Panc-1 cells were cultured in collagen matrix and incubated from a range within two to four days. Results of measured fluorescence incubated for 48 hours, shown in Figure 3-3, indicated higher proliferation within the 1 mg/ml collagen concentration compared to the 3 mg/ml concentration. In this experiment, only one replicate per control was used, whereas ideally, there should have been a minimum of three replicates. Had three replicates been used, it would have been possible to exclude the value as a significant outlier from the rest of the data. The variability in this result could be attributed to several factors. These include errors in calculation, inaccuracies in pipetting, the presence of air bubbles, or the sensitivity of the resazurin assay.

However, the experiments conducted over the periods of 72 hours and 96 hours, as depicted in Figures 3-4 and 3-5 respectively, higher cell proliferation was observed in 3 mg/ml collagen compared to 1 mg/ml. However, the baseline measurements for Figure 3-4 were higher in 1 mg/ml collagen than in 3 mg/ml, which influenced the results. Additionally, the high standard deviations noted in two of the replicates in Figure 3-5 led to their exclusion from the analysis. The mechanical properties of ECM, such as viscoelasticity, have turned out to be crucial feature of cellular behavior and the overall structure and function of both healthy and diseased tissues, including cancer (46). As mentioned earlier, one study found that with an increase in collagen I in the ECM, the pancreatic cancer cells altered the metabolism. This indicated that an increase in collagen density modifies metabolic routes and nutritional needs of these cancer cells (25). The findings from this study support the result found in these experiments, indicating that collagen density affects cell behavior, particularly Collagen I, which is the type of collagen in Telocol-10 that was used in 3D culturing during this project.

Potential sources of error in the 3D collagen experiments may include the inherent sensitivity of the resazurin assay and the formation of air bubbles within both the collagen matrix and the resazurin assay, which could have impacted the measurements and cell proliferation. Human errors, such as inaccuracies in pipetting and calculation mistakes, might have introduced variability into the results. Additionally, errors in the dilution of collagen solutions could have led to inconsistencies across the experimental setup. The limited number of replicates performed have reduced the statistical robustness of the study, thus hindering the ability to draw definitive conclusions. Furthermore, fluctuations in pH levels throughout the course of the experiments might have adversely affected the overall results.

4.3.2 The Impact of Alginate Matrices on the Growth of Panc-1

Panc-1 cells were cultured within alginate matrices and incubated over a period ranging from one to four days. Figures 3-7, 3-8. 3-9, and 3-10 all show a clearer trend observed in the alginate matrices compared to those made of collagen. A recurring observation across the experiments was that proliferation was higher in 1 % alginate compared to 2 %. This indicate that the cells proliferate more in 1 %. One study found that the stiffness of normal pancreatic tissue is approximately 0,4 kPa, in contrast, the stiffness in PDAC increased to about 1,3 kPa (47). This indicates that hardening of the ECM affects the growth of pancreatic cancer cell. One article discussed the effects of alginate concentration on cell behavior. It mentions that viscoelastic properties of alginate, particularly those modifies to include RGD peptide, influence cell spreading, focal adhesion formation, and cellular mechanotransdcution. These effects are observed when comparing different concentrations and formulations of alginate gels (48). Variations in structural elasticity, which have been shown to affect cell differentiation and function in 3D cultures, can be regulated within a certain range by adjusting the formulation parameters (49). Hence its plausible that the alginate concentration also had an effect on cellular behavior in these experiments.

However alginate naturally lacks bioactive ligands, which prevents cell adhesion, Panc-1 cells cannot attach to it because it does not include the RGD peptide that facilitates this process (50). This have likely influenced the results, as the cells were unable to adhere to the alginate matrix. However, the matrix maintained the cells in position, allowing them to adhere to each other.

Potential sources of error that may have influenced the outcomes of these experiments include the recurrent issue of air bubbles becoming entrapped within the alginate matrix, shown in Figure 7-1 in appendix. Additionally, human errors such as inaccuracies in pipetting and calculation errors could have contributed to variability in the results. The study also faced limitations due to an insufficient number of replicates, which diminished the statistical power of the analysis and hinders the ability to draw robust conclusions.

4.4 Mechanical Properties of Alginate

Mechanical properties were tested for 1 % and 2 % alginate gels, which were used to culture Panc-1 cells. Rheological measurements were conducted to evaluate the viscoelastic properties of these alginates.

The results from the rheological data show that the average viscoelasticity for the 1% alginate gel was measured at 0.00722 kPa. In contrast, the 2% alginate gel exhibited a higher

elasticity, measured at 0.01186 kPa. These measurements suggest a marked difference in the mechanical behavior of the two gel concentrations, which is further supported by the observed values of the storage modulus (G') and loss modulus (G"), presented in Figure 3-13. The results in these measurements show a clear distinction in the mechanical properties between the two concentrations. The storage modulus (G') of the 1% alginate gel was lower, indicating reduced elasticity and a comparatively weaker gel structure.

Cells possess the capability to sense the mechanical properties of their surrounding environment. Consequently, the elastic modulus of polymer hydrogels can impact their migration, development, and differentiation. Additionally, hydrogels act as analogs for the ECM, which is known to affect cell adhesion, geometry, and proliferation within their environment (51).

Overall, these findings highlight the importance of selecting appropriate alginate concentrations based on the intended application and show that different concentrations in alginate can affect cellular behavior.

4.5 Challenges with 3D Cell Cultures and Future Perspectives

4.5.1 Methodological Challenges with 3D Cell Culture using Collagen

A recurring issue throughout the experiments with was the presence of air bubbles trapped in the both the collagen matrix. The issue with air bubbles in collagen commonly occurred during the mixing process of cells into the gel, particularly when pipetting up and down to thoroughly mix the collagen and cells. Although some bubbles could be removed with a syringe tip, not all were successfully eliminated.

Additionally, air bubbles formed in the resazurin assay after incubation, a problem that arose during the transfer of the assay to new wells on the plate using a pipette, depicted in Figure 7-2 in appendix. To resolve the issue of bubble formation in the assay, the procedure was modified to pipette out 80 µl instead of the full 100 µl of resazurin that was initially added to the collagen matrix. Centrifugation of the plate removed some of the bubbles, but it was not always possible to remove all. The presence of bubbles in both the matrix and assay may have impacted viability of the cells and the measurements of fluorescence.

Another issue at the start of the project was calculating cell concentrations. To obtain more accurate results, larger volumes needed to be used; therefore, it was most practical to dilute the original cell concentration after trypsinization.

Only three replicates per group were used in these experiments with collagen, due to the limited amount of collagen remaining and the high cost of the product. Using only three replicates can be problematic because it reduces the statistical power of the experiment, which increases the variability in the results. This makes it more challenging to draw reliable conclusion from the data.

4.5.2 Methodological Challenges with 3D Cell Culture using Alginate

In methods, there is a comprehensive description of the procedure for crosslinking alginate via covalent bonds. However, this method was ultimately not selected due to the cytotoxic effects of EDC on cells.

A recurring issue throughout the experiments was the transfer of the alginate-cell mixture into syringes without entrapping air bubbles. The technique using syringes and pipettes, as described in methods, and illustrated in Figure 2-5, significantly mitigated the bubble problem. However, during crosslinking with calcium sulfate, some bubbles invariably formed, as depicted in appendix Figure 7-1.

Another complication arose with the introduction of bubbles in the resazurin assay after incubation, which occurred when using a pipette to transfer the assay into new wells on the plate, depicted in Figure 7-2 in appendix. Centrifugation of the plates removed some of the bubbles, but it was not always possible to eliminate them entirely. The presence of bubbles in both the matrix and the assay could have potentially affected the proliferation of cells and measurements of florescence and absorbance.

Another issue encountered during experiments involved the dispensing of crosslinked alginate with cells into the wells using a 1 ml syringe. Since the protocol required adding precisely 100 µl to each well, the volume was estimated by eye, which introduced a degree of inaccuracy. Consequently, it is likely that the actual volume dispersed varied and did not consistently reach the intended 100 µl per well.

4.5.3 Future Perspectives

As mentioned earlier alginates do not contain natural ECM components like bioactive ligands and are therefore not chemically active (52). This likely impacted the results of the experiments considering alginate matrices. In further experiments, RGD should be added to observe its effect on cell proliferation.

Future studies could explore the addition of other ECM components, such as growth factors or fibronectins. This could help in understanding how these components influence the microenvironment in ECM and subsequently affect cancer cell behavior.
Another investigation that could be beneficial is testing of drug response. By investigating how changes in the stiffness of ECM affect the responsiveness of Panc-1 cells to chemotherapy and targeted therapies could provide insight into optimizing treatment based on the tumor microenvironment.

5 CONCLUSION

This thesis explored the effects of varying concentrations of collagen and alginate on the growth of the Panc-1 pancreatic cancer cell line. In the research 3D culturing techniques were used to mimic the tumor microenvironment, aiming to study the role of ECM stiffness in cancer cell dynamics. The study's findings reveal that different ECM stiffness levels influence Panc-1 cell proliferation and viability, with softer matrices generally promoting more cell proliferation. This underscores the potential of manipulating ECM properties to understand more of tumor growth.
The conclusions drawn from these findings may potentially be of importance for future research. They suggest that the mechanical properties of the ECM can be strategically altered to affect cancer cell behavior, which could potentially lead to more effective therapeutic strategies. The thesis contributes to the understanding of biomechanical interactions within tumor microenvironments, and it can provide a basis for further research that aims to use these interactions to enhance treatment results in pancreatic cancer.

6 BIBLIOGRAPHY

1. Goral V. Pancreatic Cancer: Pathogenesis and Diagnosis. Asian Pac J Cancer Prev. 2. september 2015;16(14):5619–24.
2. Arneth B. Tumor Microenvironment. Medicina (Mex). 30. desember 2019;56(1):15.
3. Larsen IK, Kjerpeseth LJ. Folkehelseinstituttet. 2023 [sitert 12. mars 2024]. Kreft. Tilgjengelig på: https://www.fhi.no/he/folkehelserapporten/ikke-smittsomme/kreft/
4. Cancer Biology | NIH Intramural Research Program [Internett]. 2022 [sitert 10. april 2024]. Tilgjengelig på: https://irp.nih.gov/our-research/scientific-focus-areas/cancer-biology
5. Lin CC, Korc M. Designer hydrogels: Shedding light on the physical chemistry of the pancreatic cancer microenvironment. Cancer Lett. 1. november 2018;436:22–7.
6. NHI.no [Internett]. 2001 [sitert 27. februar 2024]. Bukspyttkjertelkreft. Tilgjengelig på: https://nhi.no/sykdommer/kreft/magetarm-kreft/bukspyttkjertelkreft
7. Cleveland Clinic [Internett]. [sitert 9. mai 2024]. Pancreas: What It Is, How It Works & Living Without One. Tilgjengelig på: https://my.clevelandclinic.org/health/body/21743-pancreas
8. Holck P. bukspyttkjertelen. I: Store medisinske leksikon [Internett]. 2023 [sitert 27. februar 2024]. Tilgjengelig på: https://sml.snl.no/bukspyttkjertelen
9. El Sayed SA, Mukherjee S. Physiology, Pancreas. I: StatPearls [Internett]. Treasure Island (FL): StatPearls Publishing; 2024 [sitert 12. mars 2024]. Tilgjengelig på: http://www.ncbi.nlm.nih.gov/books/NBK459261/
10. Falasca M, Kim M, Casari I. Pancreatic cancer: Current research and future directions. Biochim Biophys ACTA-Rev CANCER. april 2016;1865(2):123–32.
11. Kolbeinsson HM, Chandana S, Wright GP, Chung M. Pancreatic Cancer: A Review of Current Treatment and Novel Therapies. J Invest Surg. 31. desember 2023;36(1):2129884.
12. LIBRARY RHP. Science Photo Library. [sitert 10. mai 2024]. Pancreatic adenocarcinoma, illustration - Stock Image - F032/4709. Tilgjengelig på: https://www.sciencephoto.com/media/1153348/view/pancreatic-adenocarcinoma-illustration
13. Hofsli E. bukspyttkjertelkreft. I: Store medisinske leksikon [Internett]. 2023 [sitert 27. februar 2024]. Tilgjengelig på: https://sml.snl.no/bukspyttkjertelkreft
14. Mizrahi JD, Surana R, Valle JW, Shroff RT. Pancreatic cancer. LANCET. 27. juni 2020;395(10242):2008–20.
15. Bukspyttkjertelkreft [Internett]. Kreftforeningen. 2020 [sitert 6. mars 2024]. Tilgjengelig på: https://kreftforeningen.no/om-kreft/kreftformer/bukspyttkjertelkreft/
16. Shah OJ, Singh M. Developments in pancreatic cancer surgery. Updat Surg. 1. januar 2024;76(1):17–22.
17. Nielsen MFB, Mortensen MB, Detlefsen S. Key players in pancreatic cancer-stroma interaction: Cancer-associated fibroblasts, endothelial and inflammatory cells. World J Gastroenterol. 7. mars 2016;22(9):2678–700.
18. Theocharis AD, Skandalis SS, Gialeli C, Karamanos NK. Extracellular matrix structure. Adv Drug Deliv Rev. 1. februar 2016;97:4–27.
19. LeClair RJ. Extracellular Matrix. 19. november 2021 [sitert 9. mai 2024]; Tilgjengelig på: https://pressbooks.lib.vt.edu/cellbio/chapter/extracellular-matrix/
20. Chaudhuri O, Cooper-White J, Janmey PA, Mooney DJ, Shenoy VB. The impact of extracellular matrix viscoelasticity on cellular behavior. Nature. august 2020;584(7822):535–46.
21. Wu DT, Jeffreys N, Diba M, Mooney DJ. Viscoelastic Biomaterials for Tissue Regeneration. Tissue Eng Part C Methods. 1. juli 2022;28(7):289–300.
22. Pelham RJ, Wang Y l. Cell locomotion and focal adhesions are regulated by substrate

flexibility. Proc Natl Acad Sci U S A. 9. desember 1997;94(25):13661–5.
23. Yi B, Xu Q, Liu W. An overview of substrate stiffness guided cellular response and its applications in tissue regeneration. Bioact Mater. 1. september 2022;15:82–102.
24. Hosein AN, Brekken RA, Maitra A. Pancreatic cancer stroma: an update on therapeutic targeting strategies. Nat Rev Gastroenterol Hepatol. august 2020;17(8):487–505.
25. Tavares-Valente D, Cannone S, Greco MR, Carvalho TMA, Baltazar F, Queirós O, mfl. Extracellular Matrix Collagen I Differentially Regulates the Metabolic Plasticity of Pancreatic Ductal Adenocarcinoma Parenchymal Cell and Cancer Stem Cell. Cancers. 29. juli 2023;15(15):3868.
26. Armstrong T, Packham G, Murphy LB, Bateman AC, Conti JA, Fine DR, mfl. Type I Collagen Promotes the Malignant Phenotype of Pancreatic Ductal Adenocarcinoma. Clin Cancer Res. 8. november 2004;10(21):7427–37.
27. Vennin C, Murphy KJ, Morton JP, Cox TR, Pajic M, Timpson P. Reshaping the Tumor Stroma for Treatment of Pancreatic Cancer. GASTROENTEROLOGY. mars 2018;154(4):820–38.
28. Waghray M, Yalamanchili M, Magliano MPD, Simeone DM. Deciphering the role of stroma in pancreatic cancer: Curr Opin Gastroenterol. september 2013;29(5):537–43.
29. Andersen T, Auk-Emblem P, Dornish M. 3D Cell Culture in Alginate Hydrogels. Microarrays. juni 2015;4(2):133–61.
30. Sayde T, El Hamoui O, Alies B, Gaudin K, Lespes G, Battu S. Biomaterials for Three-Dimensional Cell Culture: From Applications in Oncology to Nanotechnology. Nanomaterials. 13. februar 2021;11:481.
31. Fatemeh yarmohammadi, Hayes W, Najafi N, Karimi G. The protective effect of natural compounds against rotenone-induced neurotoxicity - Yarmohammadi - 2020 - Journal of Biochemical and Molecular Toxicology - Wiley Online Library [Internett]. [sitert 12. mai 2024]. Tilgjengelig på: https://onlinelibrary-wiley-com.ezproxy.uis.no/doi/10.1002/jbt.22605
32. Abka-khajouei R, Tounsi L, Shahabi N, Patel AK, Abdelkafi S, Michaud P. Structures, Properties and Applications of Alginates. Mar Drugs. 29. mai 2022;20(6):364.
33. Baruffaldi D, Palmara G, Pirri C, Frascella F. 3D Cell Culture: Recent Development in Materials with Tunable Stiffness. ACS Appl Bio Mater. 15. mars 2021;4(3):2233–50.
34. Chaudhuri O. Viscoelastic hydrogels for 3D cell culture. Biomater Sci. 25. juli 2017;5(8):1480–90.
35. Hameed P, Manivasagam G. An overview of bio-actuation in collagen hydrogels: a mechanobiological phenomenon. Biophys Rev. 20. mai 2021;13(3):387–403.
36. Liu K, Wiendels M, Yuan H, Ruan C, Kouwer PHJ. Cell-matrix reciprocity in 3D culture models with nonlinear elasticity. Bioact Mater. 14. august 2021;9:316–31.
37. Advanced BioMatrix - Home [Internett]. [sitert 13. mai 2024]. Tilgjengelig på: https://advancedbiomatrix.com/
38. Drzewiecki K, Grisham D, Parmar A, Nanda V, Shreiber D. Circular Dichroism Spectroscopy of Collagen Fibrillogenesis: A New Use for an Old Technique. Biophys J. 1. desember 2016;111:2377–86.
39. Matinfar A, Dezfulian M, Haghighipour N, Kurdtabar M, Pourbabaei AA. Replacement of Trypsin by Proteases for Medical Applications. Iran J Pharm Res IJPR. 22. august 2022;21(1):e126328.
40. Downloadable 96 Well Plate Templates [Internett]. [sitert 10. mai 2024]. Tilgjengelig på: https://www.sigmaaldrich.com/NO/en/technical-documents/technical-article/cell-culture-and-cell-culture-analysis/cell-based-assays/96-well-plate-template
41. Resazurin - an overview | ScienceDirect Topics [Internett]. [sitert 18. april 2024]. Tilgjengelig på: https://www.sciencedirect.com/topics/pharmacology-toxicology-and-pharmaceutical-science/resazurin

42. Charbonier F, Indana D, Chaudhuri O. Tuning viscoelasticity in alginate hydrogels for 3D cell culture studies. Curr Protoc. mai 2021;1(5):e124.
43. Outlier calculator [Internett]. [sitert 28. april 2024]. Tilgjengelig på: https://www.graphpad.com/quickcalcs/grubbs1/
44. Uzarski JS, DiVito MD, Wertheim JA, Miller WM. Essential Design Considerations for the Resazurin Reduction Assay to Noninvasively Quantify Cell Expansion within Perfused Extracellular Matrix Scaffolds. Biomaterials. juni 2017;129:163–75.
45. Curvello R, Kast V, Abuwarwar MH, Fletcher AL, Garnier G, Loessner D. 3D Collagen-Nanocellulose Matrices Model the Tumour Microenvironment of Pancreatic Cancer. Front Digit Health [Internett]. 2021 [sitert 12. mai 2024];3. Tilgjengelig på: https://www.ncbi.nlm.nih.gov/pmc/articles/PMC8521838/
46. Mierke CT. Viscoelasticity Acts as a Marker for Tumor Extracellular Matrix Characteristics. Front Cell Dev Biol [Internett]. 7. desember 2021 [sitert 13. mai 2024];9. Tilgjengelig på: https://www.frontiersin.org/articles/10.3389/fcell.2021.785138
47. Gündel B, Liu X, Löhr M, Heuchel R. Pancreatic Ductal Adenocarcinoma: Preclinical in vitro and ex vivo Models. Front Cell Dev Biol. 22. oktober 2021;9:741162.
48. Chaudhuri O, Cooper-White J, Janmey PA, Mooney DJ, Shenoy VB. Effects of extracellular matrix viscoelasticity on cellular behaviour. Nature. august 2020;584(7822):535–46.
49. Larsen BE, Bjørnstad J, Pettersen EO, Tønnesen HH, Melvik JE. Rheological characterization of an injectable alginate gel system. BMC Biotechnol. 6. mai 2015;15(1):29.
50. Zhang H, Cheng J, Ao Q. Preparation of Alginate-Based Biomaterials and Their Applications in Biomedicine. Mar Drugs. mai 2021;19(5):264.
51. Kaklamani G, Cheneler D, Grover LM, Adams MJ, Bowen J. Mechanical properties of alginate hydrogels manufactured using external gelation. J Mech Behav Biomed Mater. august 2014;36:135–42.
52. Chaudhuri O. Viscoelastic hydrogels for 3D cell culture. Biomater Sci. 2017;5(8):1480–90.

7 APPENDIX

7.1 POSSIBLE ERROR SOURCES IN 3D CELL CULTURING

Figure 7-1 display air bubbles entrapped within the alginate cell matrix, while Figure 7-2 illustrates bubbles observed in the resazurin assay following transfer to new plate for fluorescence measurement.

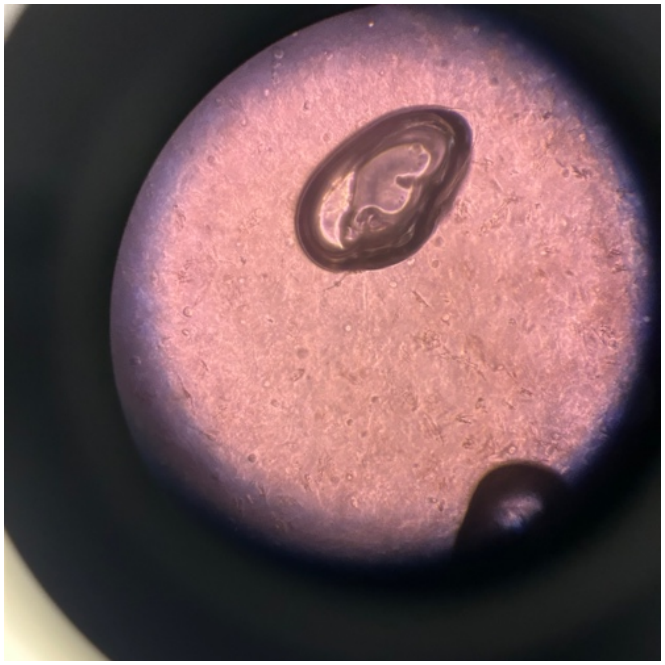

Figure 7-1: Air bubble trapped within alginate cell matrix.

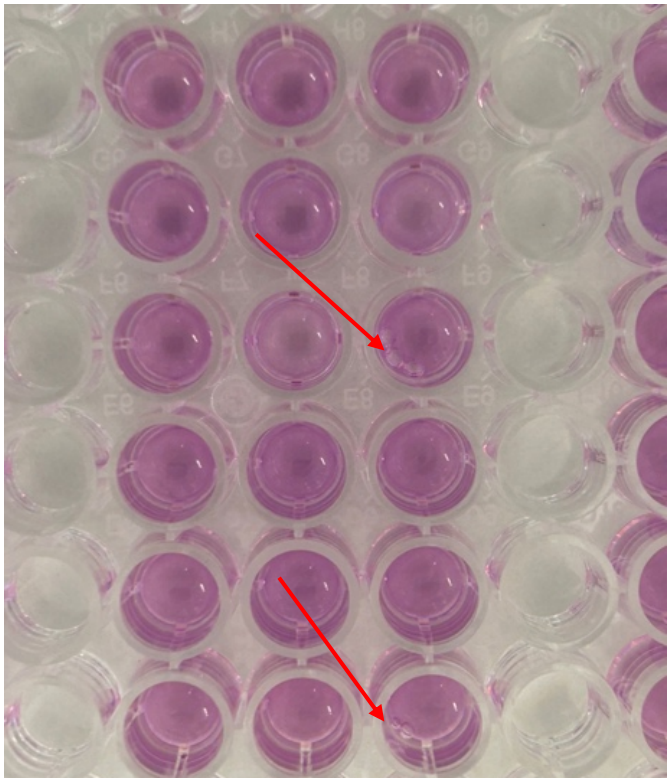

Figure 7-2: Air bubbles in resazurin assay.

7.2 Raw data for Collagen and Alginate Matrices Measured with Resazurin

7.2.1 Raw data for fluorescence and absorbance measurements in collagen

Data for fluorescence in collagen matrices presented in tables 7-1, 7-2 ,7-3,7-5 and 7-4 below. Significant outliers found in tables in are highlighted and marked in red.

Table 7-1: The raw data presents measurements of fluorescence in concentrations of cells.

24.01.2024		31.01.2024	
Number of cells	**Measured Fluorescence**	**Number of cells**	**Measured Fluorescence**
0	133572160	**0**	109660928
	120762952		123127864
	127409448		127871944
	135528112		130106512
5000	330779712	**5000**	370219936
	319802144		395651296
	335995424		346854272
	362987104		338652448
7500	262089008	**7500**	322652448
	439739040		419579488
	432524128		435686816
	382459360		394070272
10000	418259072	**10000**	549207616
	375493600		546600704
	466278112		548558912
	411009696		528869696
12500	669643904	**12500**	690997504
	567845888		714282048
	523905664		669175424
	557337600		640249984
15000	671339008	**15000**	728081792
	637236672		728803584
	643146112		736006400
	642220736		737671936
20000	667115072	**20000**	829021952
	720874112		739276224
	657157312		701886976
	657791744		662417984

Table 7-2: The raw data presents measurements of fluorescence for cells cultured in 1 mg/ml collagen and 3 mg/ml collagen and incubated for 72 hours.

04.03.2024		
Concentration collagen	Number of cells	Measured fluorescence
1 mg/ml	0	11318576
		11644143
	5000	14285279
		12233939
		14570058
	10000	15255695
		17012196
		15487416
3 mg/ml	0	8619823
		9745678
	5000	15469722
		15257913
		17041798
	10000	16785040
		17540554
		18682884

Table 7-3:The raw data presents measurements of fluorescence for cells cultured in 1 mg/ml collagen and 3 mg/ml collagen and incubated for 48 hours.

16.02.2024		
Concentration of collagen	**Number of cells**	**Measured fluorescence**
1 mg/ml	0	5347622
	5000	88100344
		68687248
		92582312
	10000	59358972
		88861328
		64148276
3 mg/ml	0	26160870
	5000	55164724
		45309192
		68725512
	10000	99609960
		67282512
		83934504

Table 7-4: The raw data presents measurements of fluorescence for cells cultured in 1 mg/ml collagen and 3 mg/ml collagen and incubated for 96 hours. Significant outlier found in measured fluorescence are marked in red.

27.02.2024		
Concentration of collagen	**Number of cells**	**Measured fluorescence**
1 mg/ml	0	9236394
		8813744
	5000	10906633
		11567820
		11072327
	10000	14894663
		13603447
		13728484
3 mg/ml	0	9269862
		9107856
	5000	11951370
		8791556
		11580068
	10000	14311896
		14617911
		13745949
12.03.2024		
Concentration of collagen	**Number of cells**	**Measured fluorescence**
1 mg/ml	0	5806302
		5124754
	5000	11407208
		5972649
		10125681
	10000	8934422
		13251513
		8836797
3 mg/ml	0	9514495
		7652943
	5000	14580566
		13426893
		11948542
	10000	17190098
		18147580
		18042568

Table 7-5: The raw data presents measurements of fluorescence for cells cultured in 1 mg/ml collagen and 3 mg/ml collagen and treated with rotenone, incubated for 72 hours.

25.03.2024		
Concentration of collagen	**5000 cells**	**Measured fluorescence**
1 mg/ml	Control	23513554
		22990128
		31121860
	Cells treated with rotenone	18357012
		24018158
		19641082
3 mg/ml	Control	22121984
		22876796
		24146922
	Cells treated with rotenone	16670000
		18060858
		17598624

7.2.2 Raw data for fluorescence and measurements in alginate

Data for fluorescence in collagen matrices presented in tables 7-6, 7-7, 7-8, and 7-9 below.

Table 7-6: The raw data presents measurements of fluorescence for cells cultured in 1 % alginate for 24 hours.

11.04.2024			
Concentration of alginate	**Number of cells**	**Measured fluorescence**	
1 %	0	12286938	8682891
		12140211	9273197
		7222274	9193990
	10000	36801608	35707760
		22993964	29136628
		33144936	26030104
		34113552	26233022
		27911404	22240138
		31047198	29953590
		30702736	29993846
		27562186	30338850
		25068924	33747220
		32990932	35114928

		24979766	42491088
		22335606	33042390
		22790068	29548250
		27261300	34046680
		27858972	28905784
		25719564	30601314
		26947794	
15.04.2024			
Concentration of alginate	**Number of cells**	**Measured fluorescence**	
1 %	0	12822592	
		11573272	
		10821068	
		9661753	
	10000	30041376	21271612
		28109654	20705286
		30800990	17619950
		33026386	18061330
		32919276	19586502
		31233604	20279364
		33478362	16888984
		31117184	21812594
		30299624	22062028
		28438500	20709964
		21169736	21334190
		22919528	24874492
		24687164	22985232
		24181044	19415578
		21096766	17051192
		17899170	18987788
		20530406	21003332
		21661278	27128146
		23539656	26681058
		22012410	23561388
		17711354	18586368
		17995374	21631446
		18261264	
		18332150	
		20083126	

Table 7-7: The raw data presents measurements of fluorescence for cells cultured in 1 % and 2 % alginate for 24 hours.

17.04.2024		
Concentration of alginate	**Number of cells**	**Measured fluorescence**
1 %	0	10069865
		10175787
		10226372
		9775970
		11462964
		10113206
	10000	22356626
		20245442
		20497334
		20903176
		20426460
		17134486
		22229764
		20784050
		16831426
		16913098
		19829896
		12965336
		18381102
		19994924
		19816668
		18015276
		17736242
		15665663
2 %	0	11447076
		11259969
		8481899
		11076335
		10441684
		11762501
	10000	19519156
		18319244
		18454568
		18654452
		18677260
		15844242
		20069152

		20733216
		21063344
		10192642
		16498590
		18740430
		18090684
		17915416
		18910128
		17276444
		12415361
		15783320

Table 7-8: The raw data presents measurements of fluorescence for cells cultured in 1 % and 2 % alginate for 48 hours.

18.04.2024		
Concentration of alginate	Number of cells	Measured fluorescence
1 %	0	10027176
		10221921
		8032588
		9773802
		9331851
		8271893
	10000	20355434
		16297748
		14881045
		15424347
		14518009
		14385798
		15687031
		16530167
		15384291
		16058985
		15604025
		18047542
		19471358
		22302236
		20599630
2 %	0	10652820
		7499224
		8592068

		8712445
		8222790
		8487125
	10000	15961258
		16603836
		13451010
		13734026
		15406350
		14387215
		17584666
		15170162
		15350407
		14921760
		17092602
		16801182
		17860218
		16021526
		14577860

Table 7-9: The raw data presents measurements of fluorescence for cells cultured in 1 % and 2 % alginate for 96 hours.

Plate 1 22.04.24			
Concentration of alginate	**Number of cells**	**Measured fluorescence**	
1 %	0	9697876	10928383
		8868578	9513099
		9658819	9656764
	10000	18706898	15462509
		13854925	17092510
		16957992	12489130
		17047040	12430988
		17684108	12512330
		15139227	12621794
		17913206	13203863
		14601894	11020010
		15801690	18029692
2 %	0	10833053	10656392
		10907126	7922676
		10933046	10464184

	10000	14908017	16463725
		17841964	17515732
		17620662	17260350
		17397412	16291857
		18594024	12149498
		18104076	15113833
		16458765	15067805
		17028528	15626984
		17137620	16336503
Plate 2 22.04.24			
Concentration of alginate	**Number of cells**	**Measured fluorescence**	
1 %	0	10464985	9986287
		10104977	11251678
		10370479	8533678
	10000	21488002	11906267
		17480924	13348903
		19943722	14133193
		18882538	18324494
		16649754	16300534
		16035224	16081065
		15590370	18300372
		14498840	16270542
		13663689	18818910
2 %	0	10398011	10009579
		11079822	9340588
		10965655	10590329
	10000	14088158	12818193
		16488735	13391705
		14710899	13574616
		12155899	13763932
		12985222	10991859
		13023898	17238176
		12253932	17153540
		12374310	16635241
		13542681	13295629

7.3 RHEOLOGIC PROPERTIES OF ALGINATE

Presented below are the raw data in 5 parallels of 1 % and 2 % depicted in graphs, Figures 7-3, and 7-4.

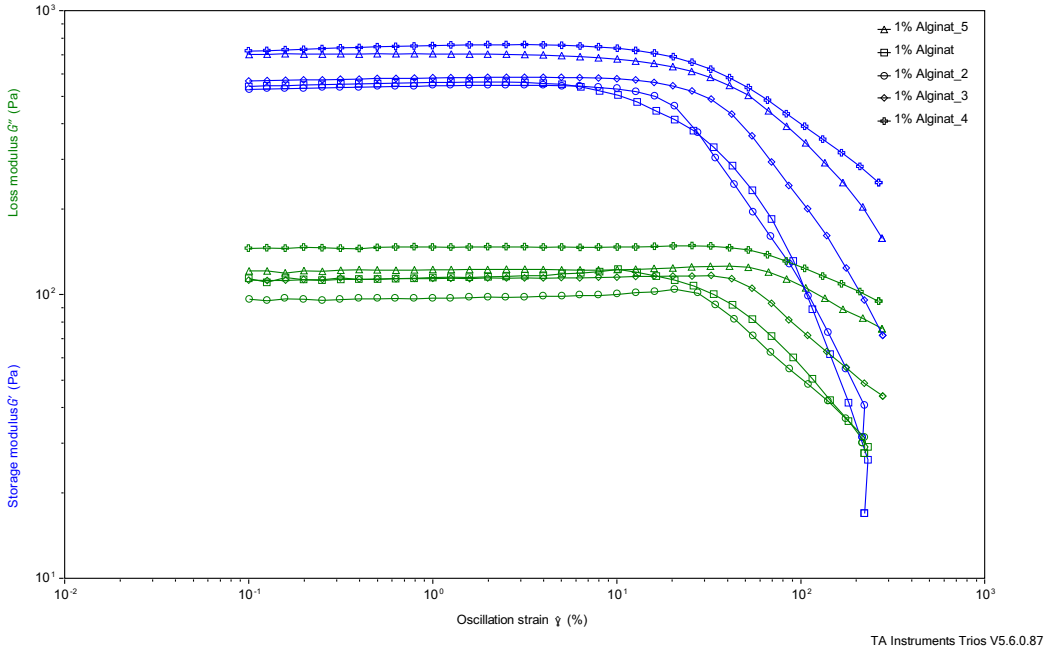

Figure 7-3: These graphs show storage modulus and loss modulus in 5 parallels of 1 % alginate gel. Storage modulus (G') measures the materials elasticity and describes how much energy is stored in the material during deformation. Loss modulus (G") measures the materials viscosity and describes how much energy is lost as heat when the material is deformed.

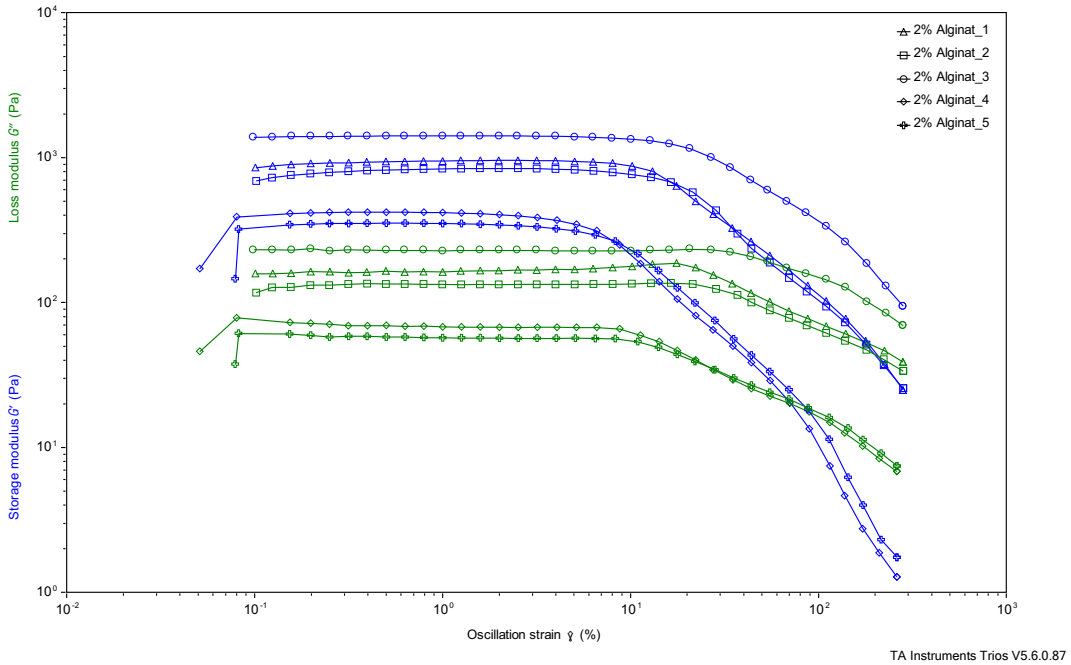

Figure 7-4: These graphs show storage modulus and loss modulus in 5 parallels of 2 % alginate gel. Storage modulus (G') measures the materials elasticity and describes how much energy is stored in the material during deformation. Loss modulus (G") measures the materials viscosity and describes how much energy is lost as heat when the material is deformed.